Estimating the density dependence of stage-specific survival and fecundity using Integrated Population Models

Christie Le Coeur[1,*], Marcel E. Visser[2], and Frédéric Barraquand[1]

[1]Institute of Mathematics of Bordeaux, CNRS & University of Bordeaux, Talence, France
[2]Department of Animal Ecology, Netherlands Institute of Ecology (NIOO-KNAW), The Netherlands

Abstract

The density dependence of survival and reproduction parameters can change with age or stage, which is key to understand population regulation mechanisms. However, the multiplication of parameters in structured demographic models makes their estimation challenging. Integrated population models (IPMs) provide an interesting solution to this issue by combining different data sources. IPM simulation studies have so far shown reliable estimates of density dependence in two-stage models, but little is known about estimation quality in more complex demographic models. Here, we used simulations to assess the bias and precision of density dependence estimates in three- and four-stage models, motivated by the life history of the great tit (*Parus major*) and a 52-year population survey. Specifically, we examined the effects of study duration (15, 30 or 50 years, on both simulated and real data), strength of density dependence, number of density-dependent parameters, temporal trend, and model structure (three versus four stages). Overall, IPMs estimated the strength of density dependence with no to little bias, but with low precision, especially when some stages were density-independent. Estimation performance improved naturally with increasing study duration, but reliable estimates were obtained starting at 30-year monitoring despite the multiplicity of data sources, suggesting simpler stage structures for shorter durations. We also showed that density-dependence was easier to detect in stable and increasing populations than in declining populations. These findings highlight the value of IPMs for assessing density dependence in structured populations, while emphasizing the need for careful model choice and interpretation given available data.

Keywords: population regulation; great tit; age structure; matrix population model; capture-mark-recapture

* Corresponding author: Christie Le Coeur, email: christielecoeur@gmail.com

1 Introduction

Estimating the effects of density dependence on demographic parameters (e.g., survival, fecundity) or population growth rate provides essential information for modelling population trajectories, assessing extinction risk and population viability, and understanding the mechanisms underlying population persistence and recovery, making it particularly important for informing management (e.g., Guthery & Shaw, 2013; Walters et al., 2026) and conservation actions (e.g., Bretagnolle et al., 2008; Margalida et al., 2020). The typically negative relationships between demographic parameters and population density shape how population growth rate varies with density (Coulson et al., 2008), thereby underpinning population regulation and providing insight into the demographic mechanisms driving it.

However, ecological time series of abundance are relatively short from a statistical standpoint, which limits the information available for inference and creates a great incentive to capitalize on all available data (Lebreton & Gimenez, 2013), including capture-recapture and reproduction data. Integrated population models (IPMs) are powerful tools to realize such fusion (Schaub & Kéry, 2021). By incorporating multiple datasets into a single framework, IPMs allow to jointly estimate density-dependent effects on multiple demographic parameters and population size, while accounting for observation errors, as well as environmental and demographic stochasticity. Several studies relied on IPMs to quantify the strength of density dependence on demographic parameters (Abadi et al., 2012; Schaub & Kéry, 2021), to investigate the demographic mechanisms underlying density-dependent population regulation (e.g., Lewis et al., 2024; Margalida et al., 2020), intraspecific and interspecific density dependence (e.g., Paquet & Barraquand, 2023; Péron & Koons, 2012; Quéroué et al., 2021); or compensatory mechanisms, in particular among harvested populations (e.g., Arnold et al., 2018; Riecke et al., 2022).

In most of these applications, density dependence was quantified directly within the IPM framework by explicitly linking demographic parameters to the estimated population size. However, this approach is increasingly challenging as model complexity rises, because it can lead to overparameterization due to the multiple life stages and parameters likely to be density-dependent. For instance, recent work has shown that in multispecies two-stage competition models, density-dependence coefficients are difficult to estimate (Paquet & Barraquand, 2025). Alternatively, density dependence effects on demographic parameters have been assessed using a two-step, *a posteriori* approach by first fitting an IPM with time-varying but density-independent demographic parameters and then, regressing the estimated demographic parameters on estimated population size (e.g., Brommer et al., 2017; Gamelon et al., 2016). This approach facilitates model fitting, but is akin to use residuals for further modelling, which is statistically frowned upon (Freckleton, 2002). It also assumes stochastic temporal variation but no temporal

autocorrelation during the IPM model fitting step, before making the opposite assumption in the density-dependence estimation step: density-dependence invariably generates temporal autocorrelation in demographic parameters because of the autocorrelation in population sizes.

Only a few studies have evaluated the bias and precision of density-dependent estimates using IPMs. While some estimates from IPMs with a simple population structure including two stages (juveniles and adults) appear reliable (Abadi et al., 2012; Paquet & Barraquand, 2023), much less is known about performance in more complex stage-structured models. Inspired by the life history and long-term monitoring of a great tit (*Parus major*) population in which density dependence has been detected at both demographic parameter and population levels (Gamelon et al., 2016; Gamelon et al., 2023; Reed, Grøtan, et al., 2013), we conducted a simulation study to assess accuracy and precision in the estimates of the strength of density dependence on stage-specific survival and fecundity, when the population is structured in three or four age-related stages. We built an IPM that combines different sources of demographic information, including capture-recapture data, annual count of breeding females, and annual count of offspring at ringing. In particular, we examined how the study duration, the value of the simulated strength of density dependence, the number of stages affected by density dependence, the temporal trend of the population (stable, increasing, or decreasing) and the stage structure of the population model (three or four) influence the bias and precision of the density dependence estimates within the IPM framework. We then used the great tit population monitored at the Hoge Veluwe National Park over 52 years as a case study to examine the influence of the study duration on the precision of density dependence estimates in a wild population.

2 Materials and methods

2.1 IPM with density dependence in demographic parameters: a common structure for simulated and case-study populations

We fitted an integrated population model to jointly estimate the stage-specific, density-dependent survival and fecundity, and the population size from three datasets: the annual count of breeding females (referred to as population count, **C**), the annual number of offspring at ringing produced by breeding females (**J**) and the capture-recapture data. The datasets and IPM structure were chosen to be consistent with the monitoring and current demographic knowledge of the great tit population at Hoge Veluwe National Park (Gamelon et al., 2016; Reed, Jenouvrier, et al., 2013). The model structure follows that proposed by Gamelon et al. (2016), with some differences described in Appendix S1. The core of the IPM is a female-based, stage-structured population model including four

stages, with a pre-breeding survey. The four stages refer to breeding females of 1 year old (yearlings, i.e. second calendar year of life), 2 year old (third calendar year), 3 year old (fourth calendar year), and those aged at least 4 years (age 4+, fifth calendar year and more). Due to the dearth of older individuals (max age = 7 years, females aged 5 years or more represent less than 2% of breeding female captures), this model can reasonably be considered age-structured. The fertility coefficient of stage a (or recruitment rate; $F_{a,t}$) is the product of fecundity $f_{a,t}$ (average number of offspring produced per breeding female of stage a across all broods in year t) considering a 50:50 sex-ratio and offspring survival $s_{0,t}$ estimated from ringing to breeding at 1 year old. The stage-specific numbers of individuals in year $t+1$ ($N_{a,t+1}$) are functions of the numbers in year t ($N_{a,t}$), the stage-specific demographic parameters ($f_{a,t}$ and $s_{a,t}$) and the number of immigrants of known and unknown ages ($A_{a,t}$ and $U_{a,t}$, respectively; details are given in the subsection Case study). Female immigrants are assumed to reproduce in the year they arrive. Immigrants of unknown age were assigned stages each year as the product of the annual stage distribution of locally born females recruiting into the population and the total number of female immigrants of unknown age that year (see computer codes). To account for demographic stochasticity, we modelled births using a Poisson distribution and survival processes according to binomial distributions. The local dynamics are obtained as follows:

$$\begin{aligned} N_{l,1,t+1} \sim \text{Poisson}(N_{1,t}s_{0,t}\frac{f_{1,t}}{2} + N_{2,t}s_{0,t}\frac{f_{2,t}}{2} + N_{3,t}s_{0,t}\frac{f_{3,t}}{2} + N_{4^+,t}s_{0,t}\frac{f_{4^+,t}}{2}) \\ N_{l,2,t+1} \sim \text{Binomial}(N_{1,t}, s_{1,t}) \\ N_{l,3,t+1} \sim \text{Binomial}(N_{2,t}, s_{2,t}) \\ N_{l,4,t+1} \sim \text{Binomial}(N_{3,t}, s_{3,t}) \\ N_{l,4^+,t+1} \sim \text{Binomial}(N_{4^+,t}, s_{4^+,t}) \end{aligned} \quad (1)$$

where l stands for 'locals', and the total number of individuals at time $t+1$ can then be obtained by adding immigrants:

$$\begin{aligned} N_{1,t+1} &= N_{l,1,t+1} + U_{1,t+1} + A_{1,t+1} \\ N_{2,t+1} &= N_{l,2,t+1} + U_{2,t+1} + A_{2,t+1} \\ N_{3,t+1} &= N_{l,3,t+1} + U_{3,t+1} + A_{3,t+1} \\ N_{4^+,t+1} &= N_{l,4,t+1} + N_{l,4^+,t+1} + U_{4^+,t+1} + A_{4^+,t+1}. \end{aligned} \quad (2)$$

We modelled the strength of density dependence on demographic parameters using logit and log links for survival and fecundity:

$$\begin{aligned} \text{logit}(s_{a,t}) &= \alpha_{s,a} + \beta_{s,a}(N_t - \bar{C}) + \varepsilon_{s,a,t}, \text{ with } \varepsilon_{s,a,t} \sim \mathcal{N}(0, \sigma^2_{s,a}) \\ \log(f_{a,t}) &= \alpha_{f,a} + \beta_{f,a}(N_t - \bar{C}) + \varepsilon_{f,a,t}, \text{ with } \varepsilon_{f,a,t} \sim \mathcal{N}(0, \sigma^2_{f,a}) \end{aligned} \quad (3)$$

with $\alpha_{s,a}$ and $\alpha_{f,a}$ the intercepts, and $\beta_{s,a}$ and $\beta_{f,a}$ the strengths of density dependence on stage-specific survival and fecundity, respectively. $\varepsilon_{s,a,t}$ and $\varepsilon_{f,a,t}$ are the uncorrelated residual errors with variance $\sigma^2_{s,a}$ and $\sigma^2_{f,a}$ (on logit scale). We subtract the mean observed population count $\bar{C}$ from the estimated population size N_t (breeding females only) to ease convergence (Schaub & Kéry, 2021).

The population count C_t corresponds to the total number of local and immigrant breeding females in the population in year t. These observed counts are related to true population size as:

$$C_t \sim \text{Normal}(N_{1,t} + N_{2,t} + N_{3,t} + N_{4^+,t}, \sigma^2) \tag{4}$$

truncated to positive values, with σ^2 the observation error variance. The model for counts is therefore a state-space (SS) model.

The annual number of ringed offspring produced by breeding females $J_{a,t}$ was used in a Poisson regression model to estimate the average annual fecundity per stage ($f_{a,t}$) as:

$$J_{a,t} \sim \text{Poisson}(f_{a,t} \times B_{a,t}) \tag{5}$$

with $B_{a,t}$ the annual count of breeding females of known age.

For capture-recapture data, we adopted a Cormack-Jolly-Seber model with an annual time step and summarized capture histories of locally ringed females as chicks and immigrants of known age in five stage-specific m-arrays ($\mathbf{m}$; Kéry and Schaub, 2012). A multinomial likelihood was used to relate the data with the apparent survival and recapture probability. Recapture probability is assumed to vary with time.

The likelihood of the IPM is defined as the joint likelihood composed of the likelihoods of the three datasets as:

$$\begin{aligned} &\mathcal{L}_{\text{IPM}}(\boldsymbol{\alpha}, \boldsymbol{\beta}, \boldsymbol{\sigma}, p, \mathbf{f}, \mathbf{s}, \mathbf{N} | \mathbf{m}, \mathbf{J}, \mathbf{C}) = \\ &\mathcal{L}_{\text{CJS}}(\boldsymbol{\alpha}_s, \boldsymbol{\beta}_s, \boldsymbol{\sigma}_s, p, \mathbf{s} | \mathbf{m}) \times \mathcal{L}_{\text{repro}}(\boldsymbol{\alpha}_f, \boldsymbol{\beta}_f, \boldsymbol{\sigma}_f, \mathbf{f} | \mathbf{J}) \times \mathcal{L}_{\text{SS}}(\boldsymbol{\alpha}, \boldsymbol{\beta}, \boldsymbol{\sigma}, p, \mathbf{f}, \mathbf{s}, \mathbf{N} | \mathbf{C}) \end{aligned}. \tag{6}$$

In some scenarios, we implemented a stage-structured population model with three stages (1-year-old, 2-year-old breeding females and those aged at least 3 years) using the same assumptions and parameterization (see code). We used the `JagsUI` package in R (Kellner, 2024) and specified weakly informative priors for all parameters (Table 1 and GitHub repository). We ran three Monte Carlo chains for 20,000 iterations, discarding the first 10,000 as burn-in and keeping every 2nd value. To assess convergence of the simulations, we used the Brooks and Gelman diagnostic $\hat{R}$ (Brooks & Gelman, 1998) and the effective size. Converged simulations were filtered by applying $\hat{R} < 1.1$ and effective sample size > 50 for all $\alpha_{s,a}$, $\alpha_{f,a}$, $\beta_{s,a}$ and $\beta_{f,a}$. Estimates are reported as posterior means and 95% credible intervals (95% CI). For each parameter, the proportion of converged

simulations in which the 95% CI contained the true parameter value was reported as the coverage probability (Appendix S2).

2.2 Scenarios

We explored bias and precision in the estimated density dependence of stage-specific demographic parameters under 21 scenarios, varying (1) the length of the time series; (2) the strength of density dependence; (3) the number of stages with density dependence; (4) the prior used for density dependence of fecundity parameters; and (5) the stage structure of the population model (Table 2; Fig. 1). Starting with a four-stage model, scenarios S1-S6 combined three lengths of time series (15, 30 and 50 years) with two strengths of density dependence in survival and fecundity (-0.01 and -0.02; Fig. 1A-B). The higher value corresponds to the strongest strength estimated among recruitment rates and survival probabilities in Gamelon et al. (2016). In scenarios S7-S9 and S11 – based on 50 years of data – the strength of density dependence in survival and fecundity was set to 0 for the two oldest stages, while it was assigned -0.01 or -0.02 for the remaining stages depending on the scenario. We applied the same combinations of density-dependence strength, number of non-zero $\beta_{s,a}$ and $\beta_{f,a}$, and time-series lengths using a three-stage structured model in Scenarios S12-S17 and S18-S19, S21 (see additional scenarios with density independence for the oldest stage only in Appendix S4, Fig. S6). In all scenarios, we assumed that all stage-specific survival rates and fecundity shared the same β value (if not set to zero). To test for prior sensitivity for $\beta_{f,a}$, we applied a normal prior distribution (S1-S9, S12-S19) or a negative exponential prior distribution (S10, S11, S20, S21). We further analyzed six scenarios where the simulated populations displayed positive (SI1-SI3) or negative temporal trends (SD1-SD3), using time series of 15 years, 30 years or 50 years, and a four-stage IPM. We hypothesized that directional trends may either improve or degrade the quality of the estimates due to changed spans of density values and, for declining populations, potential confounding between density dependent effects and temporal trend. We considered two additional scenarios for increasing and decreasing populations, based on 30 years or 50 years of monitoring, in which the strength of density dependence was set to 0 for the two oldest stages (SI4-SI5 and SD4-SD5; Appendix S5). From populations simulated over 50 years, we also examined precision and bias of density dependence in a more complex model where each stage-specific abundance can contribute to the density regulation of the stage-specific survival and fecundity (Appendix S3).

Table 1: Initial values and default parameters to simulate each of the 100 populations per scenario according to the stage structure of the population model (three or four stages). $\sigma_{f,a}$ and $\sigma_{s,a}$: temporal standard deviation of stage-specific survival and fecundity, respectively; CR: capture-recapture data; maxAge: maximum number of age classes that can be identified at first capture.

Parameters	**Four-stage model**	**Three-stage model**
Initial population vector (N_i)	$N_i = (30, 20, 20, 20)$	$N_i = (30, 20, 20)$
Maximum fecundity per stage ($f_{\max}$)	$f_{\max} = (14, 14, 14, 14)$	$f_{\max} = (14, 14, 14)$
Maximum survival per stage ($s_{\max}$)	$s_{\max} = (0.4, 0.9, 0.9, 0.8, 0.8)$	$s_{\max} = (0.4, 0.9, 0.9, 0.8)$
$\sigma_{f,a}$ and $\sigma_{s,a}$	$\sigma_{f,a} = 0.5$, $\sigma_{s,a} = 0.4$	
Breeding probability and sex-ratio	$p_{\text{Breed}} = 0.9$, sex-ratio $= 0.5$	
Probability to find a brood	0.8	
CR – Initial capture probability	0.7	
CR – Annual recapture probability (p)	$p \sim \text{Uniform}(0.7, 0.9)$	
CR – maxAge	5	4

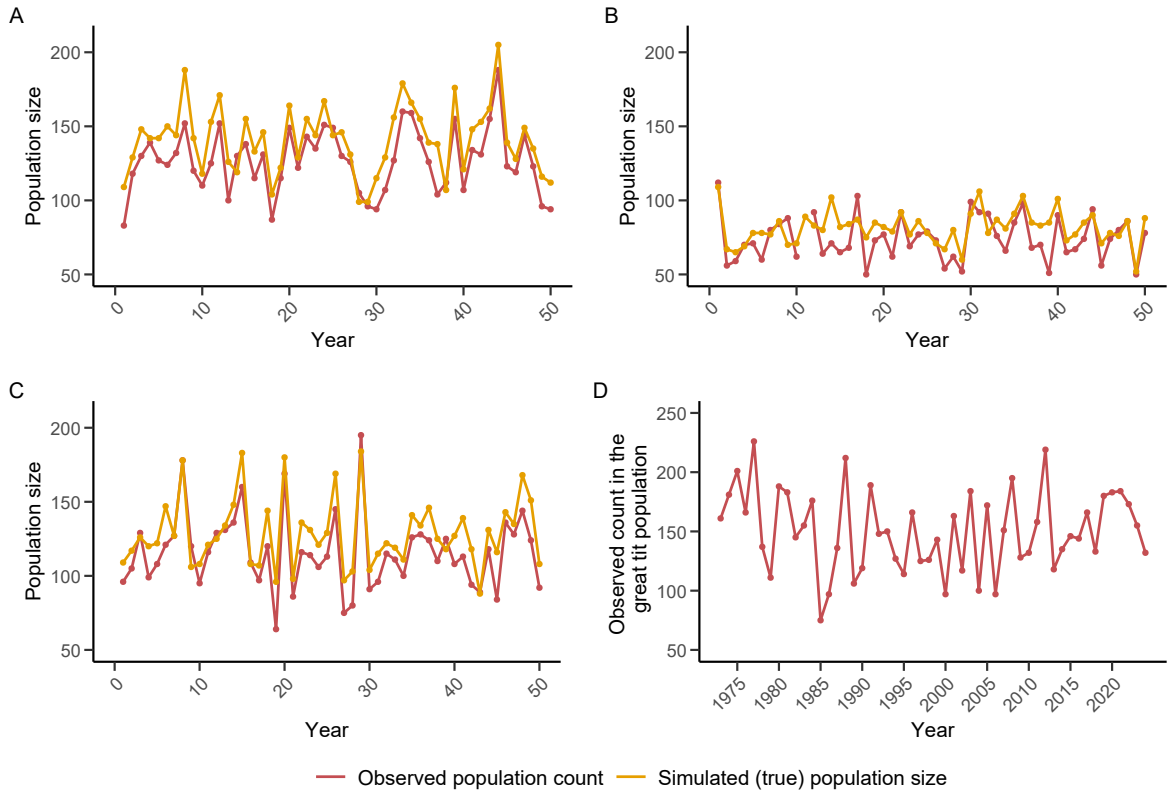

Figure 1: **A-C.** Examples of population trajectories (breeding females only) simulated for Scenarios S3, S6 and S9. In Scenarios S3 and S6 (panels A and B), density-dependence was simulated in all stage-specific demographic parameters with a strength of -0.01 and -0.02, respectively. In scenario S9 (panel C), density dependence was set to zero for the demographic parameters of the two last stages. The strength of density dependence was simulated to -0.02 for the other stages. **D.** Annual fluctuation of the observed population count (breeding females only) in the great tit population monitored at Hoge Veluwe National Park in The Netherlands.

Table 2: List of the 21 scenarios considered for the simulated populations. Scenarios varied according to the structure of the population model (three or four stages), the time series length (15, 30 or 50 years), the strength of density-dependence $\beta_{s,a}$ and $\beta_{f,a}$ (-0.02 or -0.01), the number of stages with density-dependence set to zero (0 or 2, for the two oldest stages) and the prior used for $\beta_{f,a}$. We assumed either $\beta_{f,a} \sim \mathcal{N}(0, 1)$ or $\beta_{f,a} = -\theta_a$, with $\theta_a \sim \text{Exp}(1)$ as priors. In scenarios S10 and S21 with density dependence set to 0 for two stages, $\beta_{f,a} = -\theta_a + 0.05$ was applied to include 0 in the prior distribution. DD: density dependence.

Scenarios	**Stage structure of the model**	**Time series length (in years)**	**DD strength**	**N. stages with DD set to 0**	**Prior for $\beta_{f,a}$**
S1	4	15	-0.01	0	$\mathcal{N}(0, 1)$
S2	4	30	-0.01	0	$\mathcal{N}(0, 1)$
S3	4	50	-0.01	0	$\mathcal{N}(0, 1)$
S4	4	15	-0.02	0	$\mathcal{N}(0, 1)$
S5	4	30	-0.02	0	$\mathcal{N}(0, 1)$
S6	4	50	-0.02	0	$\mathcal{N}(0, 1)$
S7	4	50	-0.01	2	$\mathcal{N}(0, 1)$
S8	4	30	-0.02	2	$\mathcal{N}(0, 1)$
S9	4	50	-0.02	2	$\mathcal{N}(0, 1)$
S10	4	50	-0.02	0	Exp(1)
S11	4	50	-0.02	2	Exp(1)
S12	3	15	-0.01	0	$\mathcal{N}(0, 1)$
S13	3	30	-0.01	0	$\mathcal{N}(0, 1)$
S14	3	50	-0.01	0	$\mathcal{N}(0, 1)$
S15	3	15	-0.02	0	$\mathcal{N}(0, 1)$
S16	3	30	-0.02	0	$\mathcal{N}(0, 1)$
S17	3	50	-0.02	0	$\mathcal{N}(0, 1)$
S18	3	50	-0.01	2	$\mathcal{N}(0, 1)$
S19	3	50	-0.02	2	$\mathcal{N}(0, 1)$
S20	3	50	-0.02	0	Exp(1)
S21	3	50	-0.02	2	Exp(1)

2.3 Simulated populations

For each scenario, 100 populations were simulated using functions of the `IPMbook` package (Schaub et al., 2023) parameterized with scenario-specific parameters (Table 2) and other initial parameter values chosen for their relevance to the monitoring of the great tit population (Table 1). True annual population size, stage-dependent m-arrays, and observed counts of chicks at ringing, breeding females of known age and immigrants were produced for each simulated population. The `simpop` function was modified to simulate populations using density-dependent, stage-specific survival and fecundity (equations 3). The annual numbers of immigrants of known and unknown ages were simulated as random draws from a Poisson distribution with means of 20 and 5 individuals, respectively. Immigrants of known age were then assigned stages using a multinomial distribution,

with probabilities given by the mean annual stage proportion observed among the local great tits. Simulated populations were filtered based on $|\log \lambda_S| < 0.01$ (from time step 3) to keep only those that reached a stable dynamic state. In scenarios with increasing and decreasing populations, we adjusted the set of initial parameter values (Appendix S5) and the simulated strength of density dependence ($\beta = -0.005$). Simulated populations were filtered according to $\log \lambda_S$ (> 0.02 or < 0.02 corresponding to increasing or decreasing temporal trends, respectively), as well as whether the population size at the final time step exceeded or felt below twice the initial population size (for increasing or decreasing populations, respectively). Estimates were compared with those obtained from 30-year stable population time series simulated with the same strength of density dependence.

2.4 Case study: Additional information on data and scenarios

Breeding great tits and offspring have been monitored in nest boxes since 1955 at Hoge Veluwe National Park in the Netherlands ($52°02'N$, $5°51'E$), a mixed pine-deciduous wood of 171 ha. We focused on the study period 1973-2024 when the study area remained the same size and the number of nest boxes was approximately constant (Jantzen & Visser, 2023; Fig. 1). The population count C_t includes breeding females that were locally born as offspring (mean annual sample size $n = 36.6 \pm 16.5$ in the 52-year dataset), immigrants of known and unknown ages ($n = 71.5 \pm 16.2$ and 12.5 ± 8.9, respectively), and females with an unknown status (not identified or aged; $n = 29.9 \pm 12.5$). Offspring were ringed 7-10 days after hatchling. On average, 802.5 ± 201.1 offspring were produced annually by breeding females of known age. Among immigrants of known age, most were yearlings ($> 56\%$) and could be easily distinguished from older individuals based on plumage characteristics (Svensson, 1992). Alternatively, individuals had previously been ringed and aged at the time of capture in mist nets in the study site. Females with "Unknown" status are those that deserted the nest before ringing, or could not be caught for any other reason. Capture-recapture data were available for 3,377 breeding females of known age and 22,150 offspring ringed in the nest. In this population, the annual recapture probability is high and fluctuated between 0.87 [0.79–0.93] (95% CI) and 0.95 [0.90–0.98] during the study period. Mean annual stage-specific survival ranged from 0.23 [0.19–0.27] for females of age 4+ to 0.45 [0.42–0.48] for females of age 2, with a low offspring survival of 0.05 [0.04–0.05]. Mean annual fecundity ranged from 7.18 [7.07–7.28] to 8.10 [7.94–8.26] offspring per female of age classes 1 and 2, respectively (estimated from an IPM with stage-specific survival and fecundity and temporal random variation over 52 years).

We examined the effect of study duration (15, 30 and 52 years) and model structure (three or four stages) on the precision of density dependence estimates under six sce-

narios (SGT1-SGT3 and SGT4-SGT6 for the four- and three-stage model, respectively). Because the study period may influence the estimates, we compared four-stage models using 15-year and 30-year-long time series starting in 1973 and in 1983 (SGT1b and SGT2b). In addition, we fitted two scenarios based on 52 years of monitoring and a negative exponential prior for $\beta_{f,a}$ (SGT7 and SGT8 with a four- and three-stage model, respectively).

3 Results

3.1 Density dependence across all stage-specific demographic parameters

Based on a four-stage model and a simulated strength value of -0.02, we found accurate estimates of the strength of density dependence across all stages for both fecundity and survival, with very low bias, while precision varied with the time series length (Fig. 2A; see coverage probabilities for corresponding scenarios S4-S6 in Table S1). Most of the simulations converged, regardless of the scenarios. A gain in precision started with a 30-year time series and improved only slightly when the series length increased to 50 years (e.g., $\beta_{s,1}$ = -0.022 95%CI[-0.044; 0.001] and -0.022 [-0.037; -0.001] with a 30-year and 50-year time series, respectively). In contrast, precision is strongly reduced when the model is based on a 15-year time series and posterior means tended to be more negative (e.g., $\beta_{s,1}$ = -0.029 95%CI[-0.085; 0.038]; Fig. 2A). Under this short time-series scenario, between 64.4 and 86.7% of the converged simulations produced credible intervals for the posterior means of density dependence that overlapped zero, depending on the stage-specific demographic parameters. Positive strength estimates were also more common among the simulations (Fig. 2B). Precision and bias were not sensitive to the prior used for $\beta_{f,a}$ (Fig. 2A). We found consistent results when the simulated strength of density dependence was set to -0.01 (Fig. S1-S2 in Appendix S3). Simplifying the model structure to three stages yielded an increase in precision of the estimates for short time-series (15 years), under weaker simulated strength of density dependence (-0.01). For example, with a simulated value of -0.01 and 15-year time series, $\beta_{s,1}$ and $\beta_{f,1}$ were estimated at -0.014 [-0.036, 0.002] and -0.011 [-0.028, 0.002], respectively, using the three-stage model, compared with -0.013 [-0.038, 0.012] and -0.012 [-0.029 0.004] using the four-stage model (Fig. S1 and S3).

3.2 Density dependence set to zero for the two oldest stages

Including both density-dependent and density-independent demographic parameters in the simulations strongly reduced model convergence (<47% of the 100 simulated populations converged for scenarios S8, S9 and S11 with 30 or 50-year time series; Fig. 3A). Among converged simulations, the average posterior mean of the strength of den-

sity dependence was close to the true values (-0.02 or 0), with precision increasing for 50-year time series. However, at the level of individual converged simulation (light blue lines in Fig. 3B), posterior mean estimates of demographic parameters with a true density independence (f_{3-4+}, s_{3-4+}) remained highly variable even with long time series, highlighting the difficulty in estimating strength when the true signal is absent. For all other parameters, individual posterior mean relationships were consistent with both the average posterior mean and simulated relationships (Fig. S4). Similar patterns were observed with a three-stage IPM model, with low convergence (<27% of the 100 simulated populations converged for scenarios S19 and S21; Fig. S5).

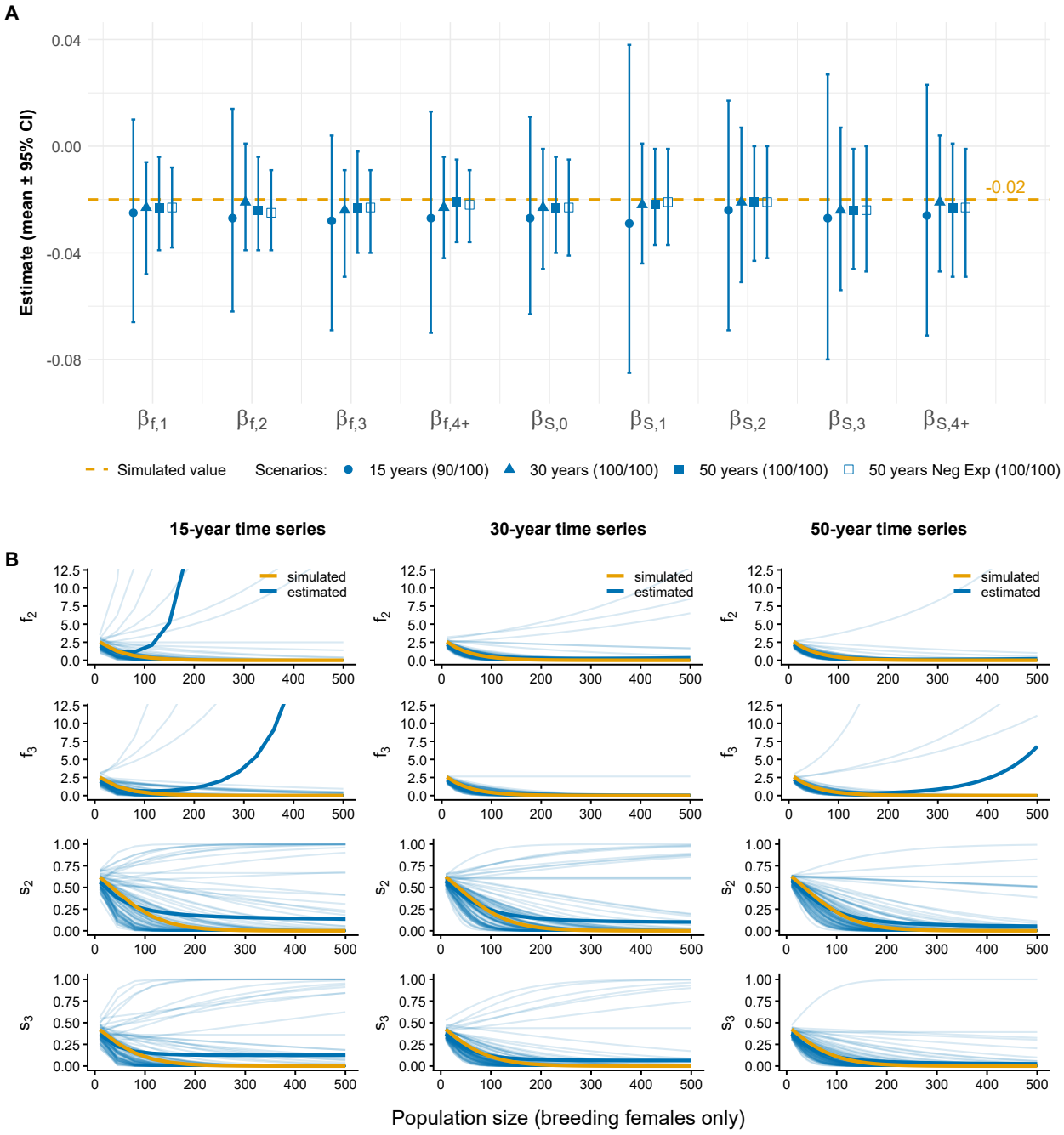

Figure 2: **A.** Average posterior means of density dependence (± 95% credible intervals) for stage-specific fecundity ($\beta_{f,1}$–$\beta_{f,4+}$) and survival ($\beta_{s,0}$–$\beta_{s,4+}$) estimated based on 15-, 30- and 50-year time series and different priors for $\beta_{f,a}$ (Scenarios S4-S6 and S10 with a four-stage model). Only converged simulations were included, with the numbers of converged populations indicated in brackets (out of 100). The simulated β value for all demographic parameters was set to -0.02 (orange dashed line). Stage classes 0-4+ correspond to offspring, yearlings, 2-year-old adults, 3-year-old adults, and adults aged $\geq$ 4 years. **B.** Density-dependent relationships for a subset of four demographic parameters (f_2, f_3, s_2 and s_3) estimated from 15-, 30- and 50-year time series (Scenarios S4-S6). Orange line: simulated relationship; Bold blue line: mean of the posterior means across all converged simulations; Light blue lines: posterior mean for each individual converged simulation.

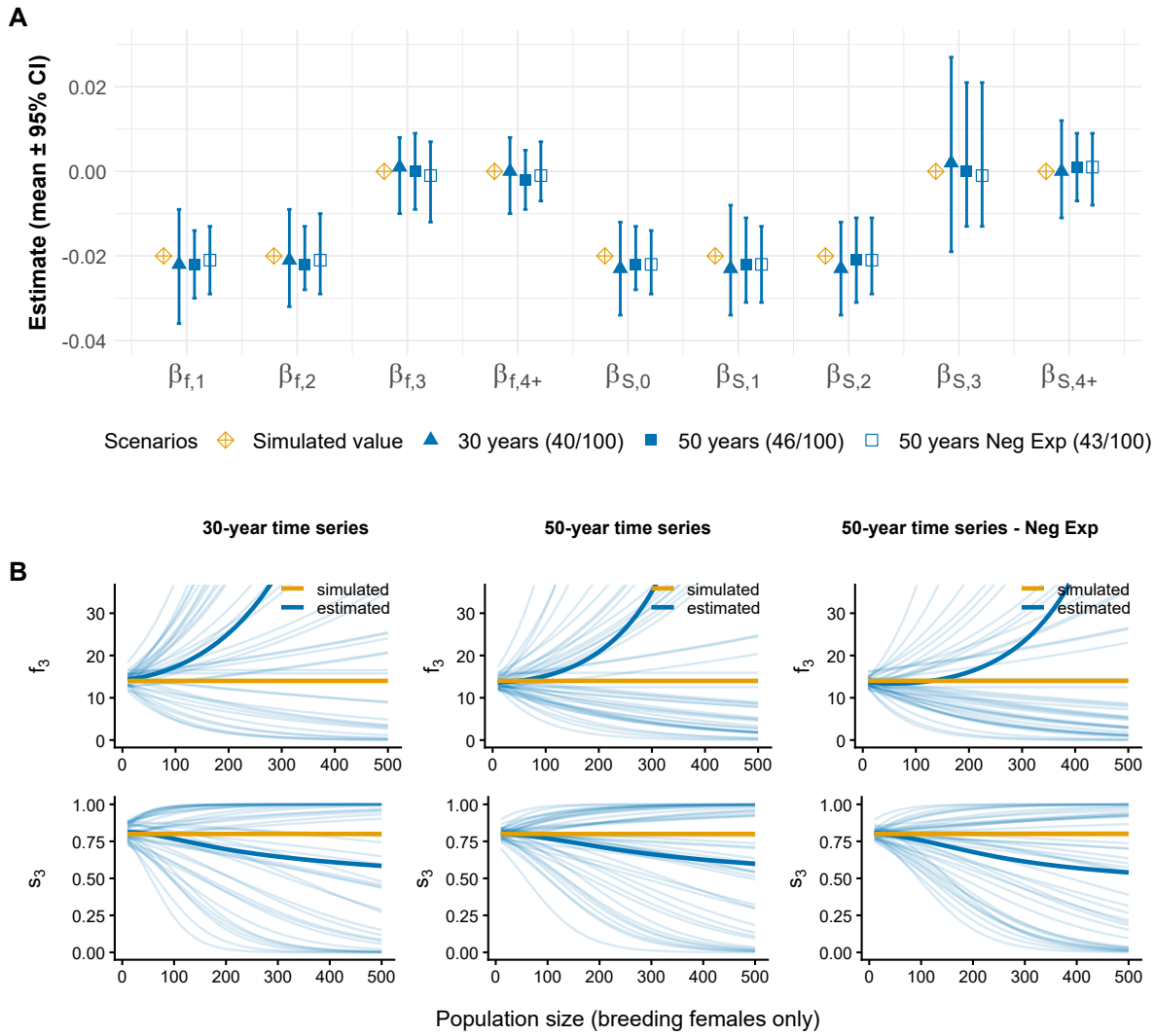

Figure 3: **A.** Average posterior mean of density dependence (± 95% credible intervals) for stage-specific fecundity ($\beta_{f,1}$–$\beta_{f,4+}$) and survival ($\beta_{s,0}$–$\beta_{s,4+}$) estimated based on 30- and 50-year time series when density dependence was set to 0 for the two oldest stages, and different priors for $\beta_{f,a}$ (Scenarios S8, S9 and S11 with a four-stage model). Only converged simulations were included, with the numbers of converged populations indicated in brackets (out of 100). The simulated β value for the demographic parameters was set to -0.02 or 0 depending on the stage (orange points). Stage classes 0-4+ correspond to offspring, yearlings, 2-year-old adults, 3-year-old adults, and adults aged $\geq$ 4 years. **B-D.** Density-dependent relationships for a subset of two demographic parameters, f_3 and s_3, for which density dependence was simulated at zero, from 30- and 50-year time series (Scenarios S8, S9 and S11). Orange line: simulated relationship; Bold blue line: mean of the posterior means across all converged simulations; Light blue lines: posterior mean for each individual converged simulation.

3.3 Increasing and decreasing populations

The temporal trend of the simulated populations influenced the precision of stage-specific density-dependence estimates (Fig. 4; Appendix S5). Precision was substantially lower when populations exhibit a decreasing trend than in those with stable or increasing trends (e.g., with a simulated value of -0.005, the average posterior means were $\beta_{s,1}$ = -0.006 [-0.035; 0.018] for declining populations; -0.006 [-0.012; -0.002] for stable populations; -0.006 [-0.013; 0.000] for increasing populations, with time series lasting 30 years; Fig. 4). Individual posterior means also showed high variability among converged simulations when populations declined over time (Fig. S8B-S9B and S11B-S12B), indicating low robustness of the estimates. As observed in previous stable population scenarios, longer time series improved estimate reliability (bias and precision) in both increasing and decreasing population scenarios.

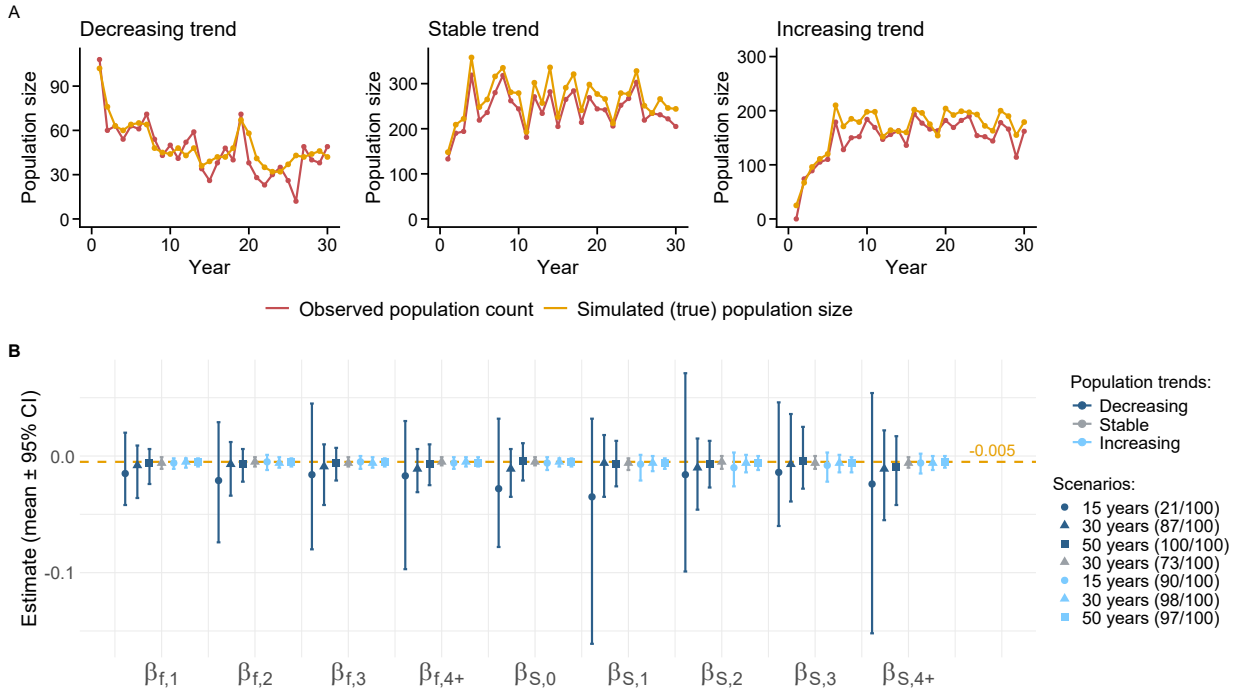

Figure 4: **A.** Examples of population trajectories showing decreasing, stable and increasing trends over 30 years, when the strength of density dependence for all stage-specific demographic parameters was simulated to be -0.005. **B.** Average posterior mean of density dependence (± 95% credible intervals) for stage-specific fecundity ($\beta_{f,1}$–$\beta_{f,4+}$) and survival ($\beta_{s,0}$–$\beta_{s,4+}$) estimated from 15-, 30-, and 50-year time series of populations with increasing or decreasing trends. Estimates were compared with those obtained from 30-year time series of stable populations (in grey). Only converged simulations were considered, with the numbers of converged populations indicated in brackets (out of 100). The simulated β value for all demographic parameters was set to -0.005 (orange dashed line). Stage classes 0-4+ correspond to offspring, yearlings, 2-year-old adults, 3-year-old adults, and adults aged $\geq$ 4 years.

3.4 Density dependence in the actual great tit population

A higher number of breeding females in the great tit population at the Hoge Veluwe National Park tends to reduce all stage-specific survival probabilities and fecundity (Fig. 5). However, the strength of density dependence varied among stages and demographic parameters. Negative density dependence was generally weaker for fecundity than for survival probabilities. Among survival probabilities, the strongest effect was observed for offspring survival, followed by survival of one- and two-year-old adult females. Consistent with the results from the simulated populations, we found that longer time series positively affected precision, with lower uncertainty for 30- and 50-year datasets. As the time series length increased, the estimated strength of density dependence in stage-specific fecundity tended to be weaker, while the negative density dependence in survival was strengthened. Similar patterns were observed with a different prior for $\beta_{f,a}$ and a simplified model structure (Appendix S6, Fig. S13).

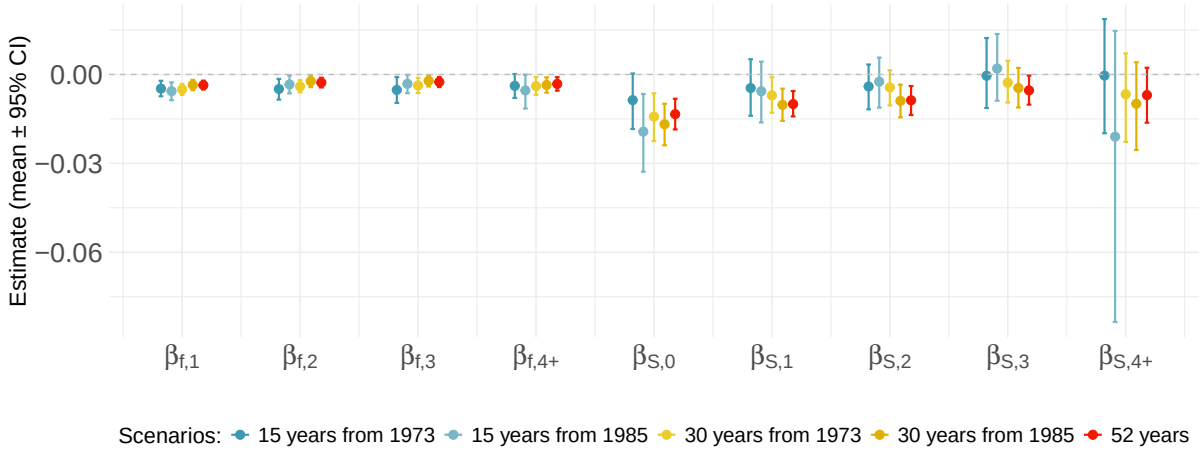

Figure 5: Posterior means of the strength of density dependence (± 95% credible intervals) in stage-specific survival probabilities ($\beta_{s,0}$-$\beta_{s,4+}$) and fecundity ($\beta_{f,1}$-$\beta_{f,4+}$) estimated in the great tit population according to the study duration and study period (scenarios SGT1-3, 1b-2b).

4 Discussion

Our simulation study shows that IPMs with log and logit links on fecundity and survival parameters generally estimate the strength of density dependence in such demographic parameters without bias. The absence of bias is evidenced by posterior means of the strength of density dependence averaged across the converged simulations, which closely match the true simulated values across all tested scenarios. However, we found that the posterior means vary substantially among the converged simulated populations (for a

given scenario), particularly (i) for density-dependent effects on survival for which heterogeneous posterior means (low precision) persist with long-term time series, and (ii) for demographic parameters where the true density-dependent effect was set to zero, with both negative and positive effects being detected. The coverage probabilities of the estimators were good (close to $1 - \alpha$), meaning that the credible intervals contained the true values for the converged fraction of the simulations: the credible intervals for density-dependence are not wrong, just broad. Broad intervals, however, can be badly interpreted in practice. One study where zero is in the credible or confidence interval may erroneously decide that density-dependence is negligible, while another may conclude to strong density-dependence while the effect is just uncertain. Such variation in the estimated strength of density dependence was already mentioned, though more briefly, in a previous simulation study using a simpler two-stage model over a 10-year study period (Abadi et al., 2012). One contribution of the present paper is therefore to show how this low precision can persist in much richer datasets with a demographic model for fast life histories that looks a bit more complicated, but not unreasonably so. We also show how study duration, population trend and the complexity of the population structure chosen in the IPM influence the bias and/or the precision of density dependence estimates. Bias decreased and precision increased with time series length, quite logically. However, the important point conveyed by our numerical experiment is that reliable estimates were obtained only starting from 30-year surveys, in spite of the large quantity of capture-recapture data complementing the counts. Moreover, increasing the time series length did not improve estimator precision when the simulated strength (density-dependence coefficient) was truly set to zero. The temporal trend (increasing, decreasing or stable) of the simulated populations also influenced the precision of the density-dependent estimates (i.e., variability in individual posterior means). With declining populations, density dependence estimates showed low precision and more bias, whereas the opposite pattern was observed with increasing populations. This can be explained by an asymmetry in logistic-like population dynamics patterns: increasing populations have first exponential growth then change convexity and saturate, so they can have a fast initial increase and still contain a lot of information about density-dependence, while decreasing populations from the same distance to equilibrium decline exponentially in a shorter time span. Survival parameters had to be modified to have visually declining populations for some time (Table S3), and the parameters compatible with such declines led to lower precision. In our particular case, increasing populations did not improve the inference anyway, which may be due to the fact that the populations already fluctuate wildly around the equilibrium (different results on increasing vs stable populations can be found when there is less "signal" in the dynamics, Barraquand and Gimenez, 2019). Precision also tended to increase when the population structure was reduced to three adult stages, particularly for short time series (15 years) and under weaker simulated density dependence (-0.01

compared to -0.02; Fig S1), suggesting that simpler structures may be preferable when data are limited. Another idea might be to use 90% credible or confidence intervals.

When the model was substantially complicated by allowing each stage to contribute differently to stage-specific density-dependent effects (Appendix S3), the IPM either failed to converge (four-stage model) or converged in only nine simulated populations (three-stage model; by increasing the number of iterations to 60,000 with a 20,000 burn-in, convergence was reached for 58 populations; see Appendix S3). In the latter case, accurate estimates of density-dependent effects were obtained solely for the influence of 1-year-old breeding females on demographic parameters. This suggests limitations in using density-dependent IPMs with full stage-by-stage density dependence matrices (a total of 21 and 34 density dependent parameters with a three- and four-stage model, respectively, instead of 7-9 in other scenarios), at least for populations with demographic features and life history similar to those of the Dutch population of great tits (i.e., given the number of ringed breeding females, population size and high recapture probability).

In the studied great tit population, we found evidence of negative density dependence in all stage-specific demographic parameters, with stronger effects on survival probabilities, especially for survival in the first year of life. These results are in line with previous studies in this population (Both et al., 1999; Gamelon et al., 2016; Reed, Jenouvrier, et al., 2013). Using either a two-step, *a posteriori* approach with an IPM (Gamelon et al., 2016) or a general framework to quantify stage contributions to density dependence in stage-structured populations (Lande et al., 2023), breeding females in their first year of reproduction (yearlings) were identified as the stage having the greatest influence on demographic parameters and population growth. Based on our simulation results, such effects appear difficult to quantify using the integrative approach (i.e., estimating density dependence directly within the IPM). In this context, comparing the integrative method and the two-step, *a posteriori* approach (i.e., estimating density dependence using regressions with estimates from a time-varying IPM) will be useful to identify the limitations of each approach, and determine which, if any, is applicable when the time series are short and/or when the number of density dependent parameters to estimate is high relative to the study duration, the mean population size and data collected. Consistent with statistical logic and the results on simulated populations, estimates and their precisions in the great tit population tended to be improved with longer time-series. 95% credible intervals excluded zero for all estimates of density dependence in stage-specific fecundity (four-stage model) from 15-year time series onward. For survival, however, credible intervals excluded zero only with time series of at least 30 years for the youngest adult stages and 50 years at least for the oldest stages (Fig. 5). This suggests that substantial monitoring is needed to parameterize stage-structured IPMs even for species with fast life histories.

Overall, IPMs can be a useful tool for quantifying density dependence of stage-specific

demographic parameters in fast-living species (e.g., small passerines and rodents). However, reliable and precise estimates require careful selection of the population structure and a sufficiently long time series. Our simulations and analyses of great tit data indicate that accurate quantification of density dependence in all stage-specific demographic parameters is only possible when long time-series (more than 20 years) from a population with stable (fluctuating) or increasing dynamics are available, and when the model structure is adapted to both the data available and the life history of the studied species. However, convergence issues and biased estimates may still arise when some stage-specific demographic parameters are truly density-independent. In our simulation framework, no individual or environmental covariate was included in the model. In the great tit population, population dynamics is known to be influenced by the combined effects of density dependence and environmental stochasticity due to annual variation in beech crops and winter temperature (Grøtan et al., 2009; Perdeck et al., 2000). Including such covariates into the model may be particularly important for quantifying both density-dependent and density-independent drivers. However, increasing model complexity by adding such covariates may affect model outcomes, in particular by reducing precision in the estimates of the strength of density dependence. At the same time, covariates may sometimes improve parameter identifiability (Cole, 2020); making it difficult to predict in which direction inserting covariates will change model performance.

In this long-term nest-box monitoring program, the annual recapture probability is high ($p_t > 0.8$), which may not be typical of other populations with similar life histories. Decreasing it (p_t simulated between 0.1 and 0.3) reduced the convergence rate and was associated with lower precision, and to a lesser extent higher bias, of stage-specific density dependence estimates for survival probabilities, while having little effect on fecundity estimates (e.g., for a simulated value of -0.02, the average posterior means for 2-year-old females were $\beta_{s,2}$ = -0.027 [-0.101; 0.039] and $\beta_{f,2}$ = -0.023 [-0.040; -0.001] in populations with low recapture probability; and $\beta_{s,2}$ = -0.021 [-0.043; 0.000] and $\beta_{f,2}$ = -0.024 [-0.039; -0.004] in populations with high recapture probability, considering 50-year time series; Fig. S14, Appendix S7). Extending our simulation approach to a wider range of life histories, particularly those with more complex stage structures or whose demographic processes are best described by multi-state capture-recapture models (e.g., slower life histories), and those with limited data (e.g., threatened or elusive species), could help provide a more comprehensive view of the potential of IPMs for investigating density-dependent effects at the demographic parameter and population levels.

Data and code availability

Code and data are available at: https://github.com/christielecoeur/Density-dependence-in-IPMs-for-fast-living-species.git

Acknowledgment

We sincerely thank everyone who contributed to the field monitoring and data collection throughout this long-term study, as well as Maartje van Deventer and Judith Risse for maintaining and sharing the long-term great tit database. We thank the board of the Hoge Veluwe National Park for permission to work in their woodlands for all these years. We are grateful to Marlène Gamelon for helpful comments on an earlier draft of this paper. This work was funded by the European Union (Marie Skłodowska-Curie grant agreement No 101149703 to CLC).

References

Abadi, F., Gimenez, O., Jakober, H., Stauber, W., Arlettaz, R., & Schaub, M. (2012). Estimating the strength of density dependence in the presence of observation errors using integrated population models. *Ecological Modelling*, *242*, 1–9. https://doi.org/10.1016/j.ecolmodel.2012.05.007

Arnold, T. W., Clark, R. G., Koons, D. N., & Schaub, M. (2018). Integrated population models facilitate ecological understanding and improved management decisions. *The Journal of Wildlife Management*, *82*(2), 266–274. https://doi.org/10.1002/jwmg.21404

Barraquand, F., & Gimenez, O. (2019). Integrating multiple data sources to fit matrix population models for interacting species. *Ecological modelling*, *411*, 108713. https://doi.org/10.1016/j.ecolmodel.2019.06.001

Both, C., Visser, M. E., & Verboven, N. (1999). Density–dependent recruitment rates in great tits: The importance of being heavier. *Proceedings of the Royal Society of London. Series B: Biological Sciences*, *266*(1418), 465–469. https://doi.org/10.1098/rspb.1999.0660

Bretagnolle, V., Mougeot, F., & Thibault, J.-C. (2008). Density dependence in a recovering osprey population: Demographic and behavioural processes. *Journal of Animal Ecology*, 998–1007. https://www.jstor.org/stable/20143276

Brommer, J. E., Wistbacka, R., & Selonen, V. (2017). Immigration ensures population survival in the Siberian flying squirrel. *Ecology and Evolution*, *7*(6), 1858–1868. https://doi.org/10.1002/ece3.2807

Brooks, S. P., & Gelman, A. (1998). General Methods for Monitoring Convergence of Iterative Simulations. *Journal of Computational and Graphical Statistics*, *7*(4), 434–455. https://doi.org/10.1080/10618600.1998.10474787

Cole, D. (2020). *Parameter redundancy and identifiability*. Chapman and Hall/CRC.

Coulson, T., Ezard, T. H. G., Pelletier, F., Tavecchia, G., Stenseth, N. C., Childs, D. Z., Pilkington, J. G., Pemberton, J. M., Kruuk, L. E. B., Clutton-Brock, T. H., & Crawley, M. J. (2008). Estimating the functional form for the density dependence from life history data. *Ecology*, *89*(6), 1661–1674. https://doi.org/10.1890/07-1099.1

Freckleton, R. P. (2002). On the misuse of residuals in ecology: Regression of residuals vs. multiple regression. *Journal of Animal Ecology*, 542–545. https://www.jstor.org/stable/2693531

Gamelon, M., Grøtan, V., Engen, S., Bjørkvoll, E., Visser, M. E., & Sæther, B.-E. (2016). Density dependence in an age-structured population of great tits: Identifying the critical age classes. *Ecology*, *97*(9), 2479–2490. https://doi.org/10.1002/ecy.1442

Gamelon, M., Jenouvrier, S., Lindner, M., Sæther, B.-E., & Visser, M. E. (2023). Detecting climate signals cascading through levels of biological organization. *Nature Climate Change*, *13*(9), 985–989. https://www.nature.com/articles/s41558-023-01760-y

Grøtan, V., Sæther, B.-E., Engen, S., Van Balen, J. H., Perdeck, A. C., & Visser, M. E. (2009). Spatial and temporal variation in the relative contribution of density dependence, climate variation and migration to fluctuations in the size of great tit populations. *Journal of Animal Ecology*, *78*(2), 447–459. https://doi.org/10.1111/j.1365-2656.2008.01488.x

Guthery, F. S., & Shaw, J. H. (2013). Density dependence: Applications in wildlife management. *The Journal of Wildlife Management*, *77*(1), 33–38. https://doi.org/10.1002/jwmg.450

Jantzen, C. C., & Visser, M. E. (2023). Climate change does not equally affect temporal patterns of natural selection on reproductive timing across populations in two songbird species. *Proceedings of the Royal Society B: Biological Sciences*, *290*(2009). https://doi.org/10.1098/rspb.2023.1474

Kellner, K. (2024). *Jagsui: A wrapper around 'rjags' to streamline 'jags' analyses* [R package version 1.6.2]. https://CRAN.R-project.org/package=jagsUI

Lande, R., Grøtan, V., Engen, S., Visser, M. E., & Sæther, B.-E. (2023). Estimating density dependence, environmental variance, and long-term selection on a stage-structured life history. *The American Naturalist*, *201*(4), 557–573. https://doi.org/10.1086/723211

Lebreton, J.-D., & Gimenez, O. (2013). Detecting and estimating density dependence in wildlife populations. *The Journal of Wildlife Management*, *77*(1), 12–23. https://doi.org/10.1002/jwmg.425

Lewis, W. B., Nater, C. R., Rectenwald, J. A., Sisson, D. C., & Martin, J. A. (2024). Use of integrated population models for assessing density-dependence and juvenile survival in Northern Bobwhites (Colinus virginianus). *PeerJ*, *12*, e18625. https://peerj.com/articles/18625/

Margalida, A., Jiménez, J., Martínez, J. M., Sesé, J. A., García-Ferré, D., Llamas, A., Razin, M., Colomer, M., & Arroyo, B. (2020). An assessment of population size and demographic drivers of the Bearded Vulture using integrated population models. *Ecological Monographs*, *90*(3), e01414. https://doi.org/10.1002/ecm.1414

Paquet, M., & Barraquand, F. (2023). Assessing species interactions using integrated predator-prey models. *Peer Community Journal*, *3*. https://peercommunityjournal.org/articles/10.24072/pcjournal.337/

Paquet, M., & Barraquand, F. (2025). *Using theory-driven Integrated Population Models to evaluate competitive outcomes in stage-structured systems*. arXiv: 2504.06725 [q-bio]. https://doi.org/10.48550/arXiv.2504.06725

Perdeck, A. C., Visser, M. E., & Van Balen, J. H. (2000). Great tit *Parus major* survival and the beech-crop cycle. *Ardea*, *88*(1), 99–108.

Péron, G., & Koons, D. N. (2012). Integrated modeling of communities: Parasitism, competition, and demographic synchrony in sympatric ducks. *Ecology*, *93*(11), 2456–2464. https://doi.org/https://doi.org/10.1890/11-1881.1

Quéroué, M., Barbraud, C., Barraquand, F., Turek, D., Delord, K., Pacoureau, N., & Gimenez, O. (2021). Multispecies integrated population model reveals bottom-up dynamics in a seabird predator–prey system. *Ecological Monographs*, *91*(3), e01459. https://doi.org/10.1002/ecm.1459

Reed, T. E., Grøtan, V., Jenouvrier, S., Sæther, B.-E., & Visser, M. E. (2013). Population growth in a wild bird is buffered against phenological mismatch. *Science*, *340*(6131), 488–491. https://doi.org/10.1126/science.1232870

Reed, T. E., Jenouvrier, S., & Visser, M. E. (2013). Phenological mismatch strongly affects individual fitness but not population demography in a woodland passerine. *Journal of Animal Ecology*, *82*(1), 131–144. https://doi.org/10.1111/j.1365-2656.2012.02020.x

Riecke, T. V., Lohman, M. G., Sedinger, B. S., Arnold, T. W., Feldheim, C. L., Koons, D. N., Rohwer, F. C., Schaub, M., Williams, P. J., & Sedinger, J. S. (2022). Density-dependence produces spurious relationships among demographic parameters in a harvested species. *Journal of Animal Ecology*, *91*(11), 2261–2272. https://doi.org/10.1111/1365-2656.13807

Schaub, M., & Kéry, M. (2021). *Integrated population models: Theory and ecological applications with R and JAGS*. Academic Press.

Schaub, M., Kéry, M., & Meredith, M. (2023). *Ipmbook: Functions and data for the book 'integrated population models'* [R package version 0.1.5]. https://CRAN.R-project.org/package=IPMbook

Svensson, L. (1992). *Identification guide to European passerines*. British Trust for Ornithology.

Walters, C. L., Gantner, N., Hagen, J., Spendlow, I., Pillipow, R., & Martins, E. G. (2026). Disentangling the contributions of density dependence and independence to population growth rates. *Ecological Applications*, *36*(2), e70199. https://doi.org/10.1002/eap.70199

Supporting information

S1. Differences between the present Integrated Population Model (IPM) and the model of Gamelon et al. (2016)

The IPM developed here builds upon the IPM presented by Gamelon et al. (2016) for the same study population. Both models are female-based, structured into four stages (breeding females of 1 year old, 2 year old, 3 year old, and those aged at least 4 years) with a pre-breeding survey, and integrating the same demographic data sources. Nevertheless, the current implementation includes several methodological modifications. The main difference between the two models lies in the analysis of density dependence of demographic parameters. In the present study, density dependence was estimated directly within the IPM framework using an integrated approach. In contrast, Gamelon et al. (2016) adopted a two-step, *a posteriori* approach, by first fitting a density-independent IPM in which demographic parameters varied through time, and then, regressing the estimated demographic parameters against the estimated population size to infer density-dependent coefficients.
Additional changes relative to the model of Gamelon et al. (2016) are outlined below:

- Juvenile capture–recapture data were incorporated into the IPM, allowing juvenile survival and its density dependence to be estimated directly within the IPM;
- We modelled density dependence of fecundity rather than of fertility (i.e., recruitment): this allows to separate effects on fecundity and juvenile survival;
- We did not include a residual variance–covariance matrix to account for correlated temporal variation among demographic parameters.

Reference: Gamelon, M., Grøtan, V., Engen, S., Bjørkvoll, E., Visser, M. E., & Sæther, B. E. (2016). Density dependence in an age-structured population of great tits: identifying the critical age classes. Ecology, 97(9), 2479-2490.

S2. Coverage probability

Table S1: Coverage probability of the density dependence estimates ($\beta_{f,a}$ and $\beta_{s,a}$) for the 21 scenarios (described in Table S2). Among the converged simulations, the coverage probability for a parameter corresponds to the proportion of simulations in which the 95% credible interval (CI) contains the true parameter value.

Scenarios	**N° of converged simulations**	$\beta_{f,1}$	$\beta_{f,2}$	$\beta_{f,3}$	$\beta_{f,4^+}$	$\beta_{s,0}$	$\beta_{s,1}$	$\beta_{s,2}$	$\beta_{s,3}$	$\beta_{s,4^+}$
S1	81	0.93	0.99	0.98	0.93	0.96	0.94	0.95	0.99	0.94
S2	97	0.92	0.93	0.91	0.96	0.94	0.93	0.95	0.96	0.95
S3	99	0.96	0.95	0.92	0.95	0.93	0.97	0.98	0.99	0.95
S4	90	0.94	0.96	0.91	0.94	0.94	0.97	0.93	0.98	0.97
S5	100	0.95	0.96	0.95	0.96	0.94	0.94	0.93	0.93	0.97
S6	100	0.94	0.97	0.93	0.98	0.96	0.96	0.95	0.96	0.94
S7	22	0.95	0.95	0.95	0.95	0.95	0.91	0.91	0.91	1.00
S8	40	0.95	0.98	0.95	0.93	0.93	0.93	0.98	0.98	1.00
S9	46	0.96	1.00	0.93	0.89	0.93	0.93	0.96	0.91	0.96
S10	100	0.97	0.99	0.95	0.99	0.95	0.96	0.95	0.95	0.94
S11	43	0.95	0.95	0.95	0.95	0.95	0.95	0.93	0.95	0.95
S12	85	0.93	0.99	0.89	-	0.96	0.91	0.95	0.95	-
S13	89	0.97	0.97	0.93	-	0.90	0.97	0.99	0.98	-
S14	93	0.91	0.90	0.94	-	0.94	0.95	0.91	0.96	-
S15	88	0.94	0.96	0.90	-	0.92	0.96	0.98	0.95	-
S16	99	0.95	0.95	0.94	-	0.94	0.91	0.97	0.91	-
S17	100	0.92	0.96	0.92	-	0.94	0.98	0.91	0.95	-
S18	7	1.00	0.86	1.00	-	1.00	0.86	1.00	0.71	-
S19	24	1.00	0.92	0.92	-	0.92	0.92	0.92	1.00	-
S20	99	0.94	0.96	0.94	-	0.94	0.96	0.90	0.95	-
S21	26	0.96	0.92	0.96	-	0.96	0.85	0.96	0.96	-

Table S2: List of the 21 scenarios. Scenarios varied according to the structure of the population model (three or four stages), the time series length, the strength of density-dependence $\beta_{s,a}$ and $\beta_{f,a}$, the number of stages with density-dependence set to zero (0 or 2, for the two oldest stages) and the prior used for $\beta_{f,a}$. We assumed either $\beta_{fa} \sim \mathcal{N}(0, 1)$ or $\beta_{fa} = -\theta_a$, with $\theta_a \sim \text{Exp}(1)$ as priors. In scenarios S10 and S21 with density dependence set to 0 for two stages, $\beta_{fa} = -\theta_a + 0.05$ was applied to include 0 in the prior distribution. DD: density dependence.

Scenarios	**Stage structure of the model**	**Time series length (in years)**	**DD strength**	**N. stages with DD set to 0**	**Prior for** $\beta_{f,a}$
S1	4	15	-0.01	0	$\mathcal{N}(0, 1)$
S2	4	30	-0.01	0	$\mathcal{N}(0, 1)$
S3	4	50	-0.01	0	$\mathcal{N}(0, 1)$
S4	4	15	-0.02	0	$\mathcal{N}(0, 1)$
S5	4	30	-0.02	0	$\mathcal{N}(0, 1)$
S6	4	50	-0.02	0	$\mathcal{N}(0, 1)$
S7	4	50	-0.01	2	$\mathcal{N}(0, 1)$
S8	4	30	-0.02	2	$\mathcal{N}(0, 1)$
S9	4	50	-0.02	2	$\mathcal{N}(0, 1)$
S10	4	50	-0.02	0	Exp(1)
S11	4	50	-0.02	2	Exp(1)
S12	3	15	-0.01	0	$\mathcal{N}(0, 1)$
S13	3	30	-0.01	0	$\mathcal{N}(0, 1)$
S14	3	50	-0.01	0	$\mathcal{N}(0, 1)$
S15	3	15	-0.02	0	$\mathcal{N}(0, 1)$
S16	3	30	-0.02	0	$\mathcal{N}(0, 1)$
S17	3	50	-0.02	0	$\mathcal{N}(0, 1)$
S18	3	50	-0.01	2	$\mathcal{N}(0, 1)$
S19	3	50	-0.02	2	$\mathcal{N}(0, 1)$
S20	3	50	-0.02	0	Exp(1)
S21	3	50	-0.02	2	Exp(1)

S3. Density dependence across all stage-specific demographic parameters

- **Comparison between scenarios when two model structures and two true (simulated) values of density dependence were applied**

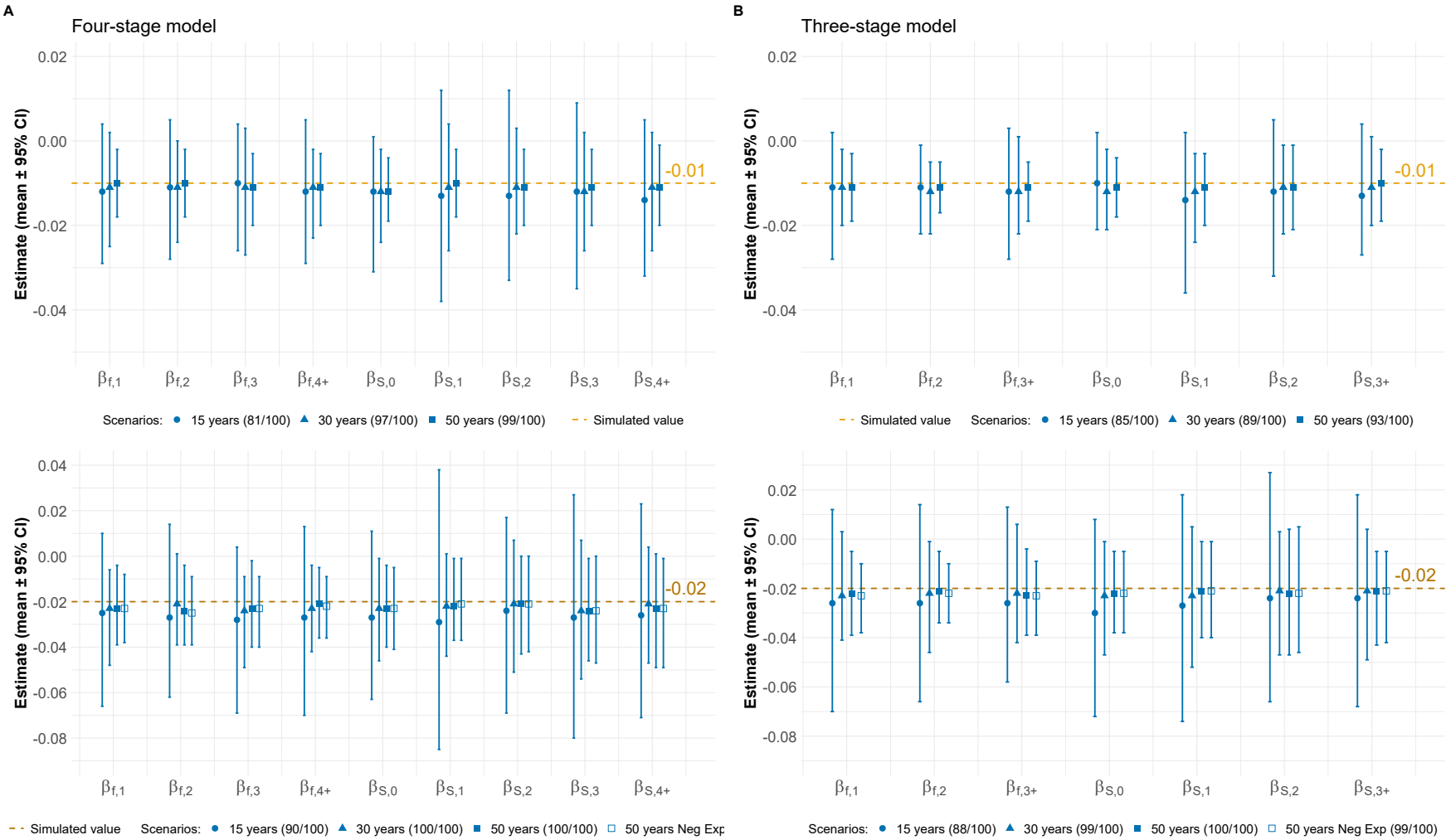

Figure S1: Average posterior means of density dependence (± 95% credible intervals) for stage-specific fecundity and survival estimated based on different model structure (**A.** four-stage models; **B.** three-stage models), different strength of density dependence (top panels: -0.01; bottom panels: -0.02; orange dashed lines: simulated strength), time series length (15-, 30- and 50-year time series) and different priors for $\beta_{f,a}$ (a normal prior or a negative exponential distribution). Only converged simulations were considered, with the numbers of converged populations indicated in brackets (out of 100) for each scenario. In a four-stage model, stages 0-4+ correspond to offspring, 1-year-old, 2-year-old, 3-year-old adults, and adults aged ≥ 4 years. In a three-stage model, stages 0-3+ are offspring, 1-year old, 2-year-old, and adults aged ≥ 3 years.

- **Scenarios S1-S3: A four-stage model with true density dependence estimates set to -0.01 for all stage-specific survival and fecundity**

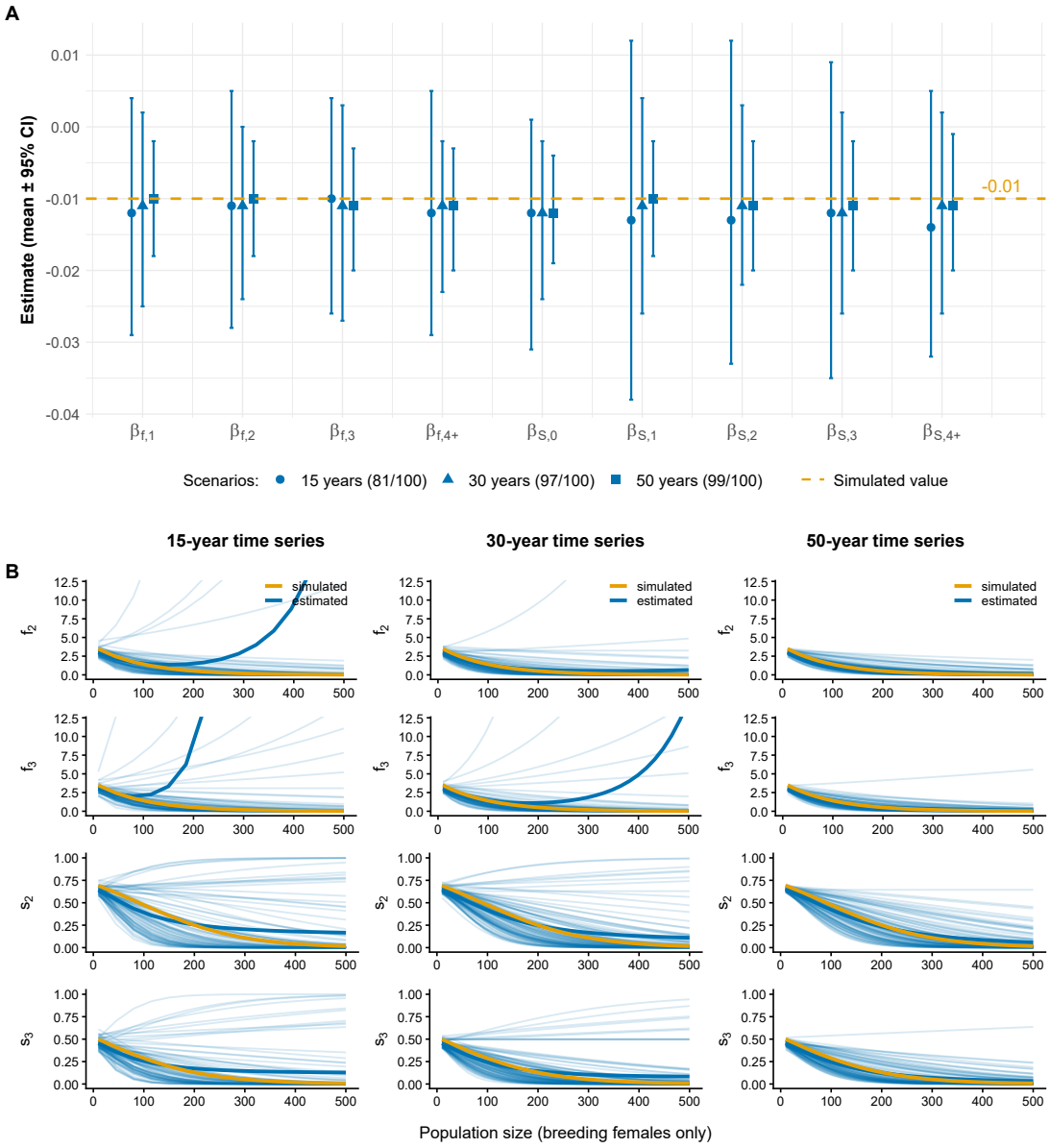

Figure S2: **A.** Average posterior means of density dependence (± 95% credible intervals) for stage-specific fecundity ($\beta_{f,1}$-$\beta_{f,4+}$) and survival ($\beta_{s,0}$-$\beta_{s,4+}$) estimated based on 15-, 30- and 50-year time series and different priors for $\beta_{f,a}$ (Scenarios S1-3 with four-stage models). Only converged simulations were included, with the numbers of converged populations indicated in brackets (out of 100). The simulated β value for all demographic parameters was set to -0.01 (orange dashed line). Stage classes 0-4+ correspond to offspring, yearlings, 2-year-old adults, 3-year-old adults, and adults aged ≥ 4 years. **B.** Density-dependent relationships for a subset of four demographic parameters (f_2, f_3, s_2 and s_3) estimated from 15-, 30- and 50-year time series. Orange line: simulated relationship; Bold blue line: mean of the posterior means across all converged simulations; Light blue lines: posterior mean for each individual converged simulation.

- **Scenarios S15-S17, S20: A three-stage model with true density dependence estimates set to -0.02 for all stage-specific survival and fecundity**

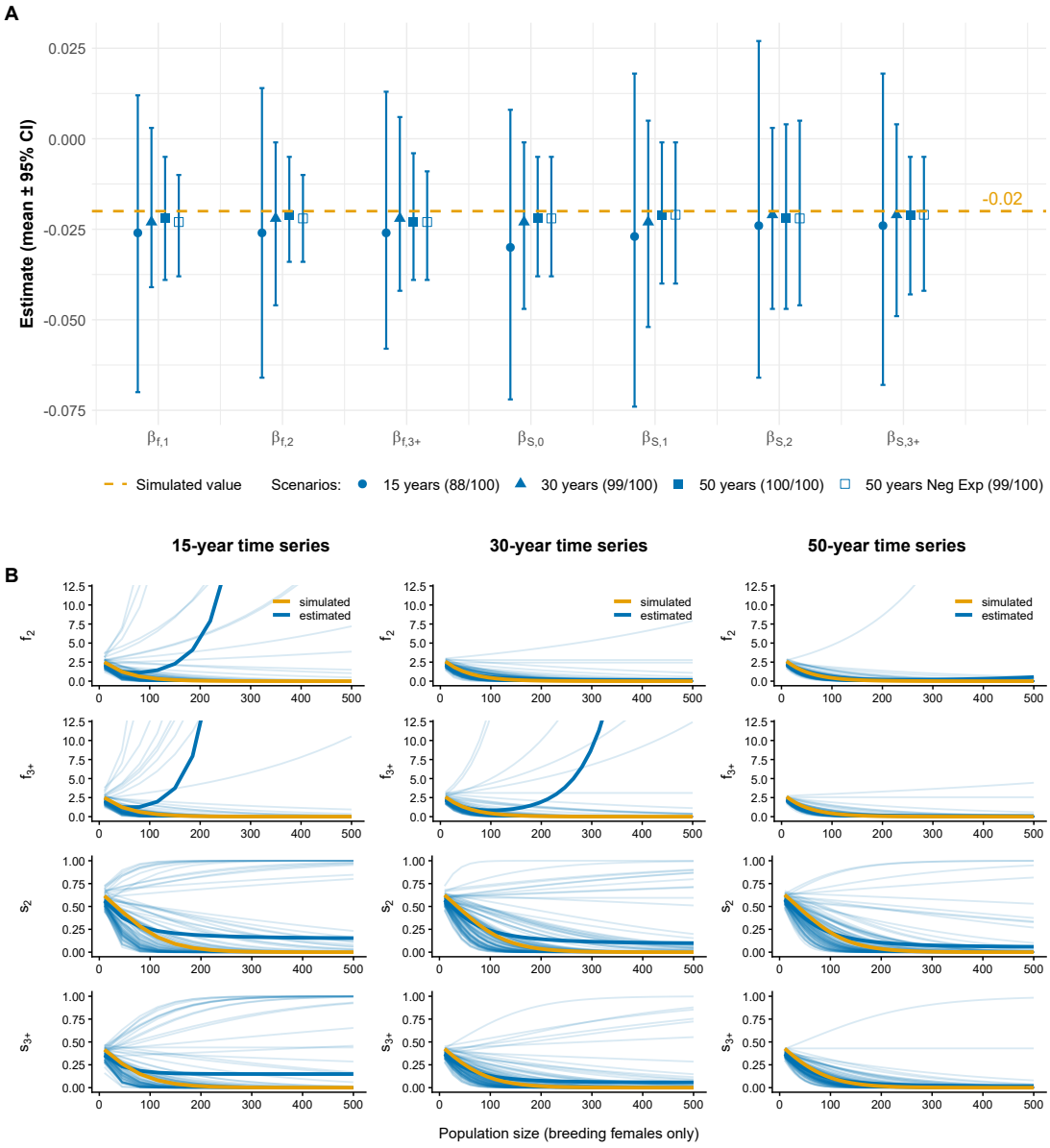

Figure S3: **A.** Average posterior means of density dependence (± 95% credible intervals) for stage-specific fecundity ($\beta_{f,1}$-$\beta_{f,3+}$) and survival ($\beta_{s,0}$-$\beta_{s,3+}$) estimated based on 15-, 30- and 50-year time series and different priors for $\beta_{f,a}$ (Scenarios S15-S17, S20 with three-stage models). Only converged simulations were included, with the numbers of converged populations indicated in brackets (out of 100). The simulated β value for all demographic parameters was set to -0.02 (orange dashed line). Stage classes 0-3+ correspond to offspring, yearlings, adults of age 2 and adults of age 3+. **B.** Density-dependent relationships for a subset of four demographic parameters (f_2, f_{3+}, s_2 and s_{3+}) estimated from 15-, 30- and 50-year time series (Scenarios S15-S17). Orange line: simulated relationship; Bold blue line: mean of the posterior means across all converged simulations; Light blue lines: posterior mean for each individual converged simulation.

- **Additional scenario: stage-specific abundances contribute to density regulation of the stage-specific survival and fecundity**

From 50-year datasets and a four-stage population model, we examined precision and bias of the strength of density dependence in a more complex model where each stage-specific abundance can contribute to the density regulation of the stage-specific survival and fecundity, as:

$$\begin{aligned} \text{logit}(s_{a,t}) &= \alpha_{s,a} + \beta_{s,a,1}N_{1,t} + \beta_{s,a,2}N_{2,t} + \beta_{s,a,3}N_{3,t} + \beta_{s,a,4^+}N_{4^+,t} + \varepsilon_{sa,t}, \\ &\text{with } \varepsilon_{s,a,t} \sim \mathcal{N}(0, \sigma^2_{s,a}) \\ \text{logit}(f_{a,t}) &= \alpha_{f,a} + \beta_{f,a,1}N_{1,t} + \beta_{f,a,2}N_{2,t} + \beta_{f,a,3}N_{3,t} + \beta_{f,a,4^+}N_{4^+,t} + \varepsilon_{fa,t}, \\ &\text{with } \varepsilon_{f,a,t} \sim \mathcal{N}(0, \sigma^2_{f,a}) \end{aligned} \tag{7}$$

We set each $\beta_{s,a,1:4^+}$ and $\beta_{s,a,1:4^+}$ to -0.02. Converged simulations were filtered by applying $\hat{R} < 1.1$ and effective sample size > 50 for all $\alpha_{s,a}$, $\alpha_{f,a}$, $\beta_{s,a,1:4^+}$ and $\beta_{f,a,1:4^+}$. Among the 100 simulated populations, none achieved convergence for all parameters.

We applied the same scenario using a three-stage model. Only nine simulations out of 100 simulated populations achieved convergence. Among the nine converged simulations, the negative effect of 1-year-old breeding females on the stage-specific demographic parameters was accurately estimated (no bias, $\beta_{s,a,1:3^+}$ and $\beta_{s,a,1:3^+}$ around -0.02). In contrast, density dependence effects of older breeding females on the stage-specific fecundity and survival were estimated to zero (instead of -0.02), with more uncertainty in $\beta_{s,a,1:3^+}$, indicating that the IPM cannot infer correctly how different stages contribute to density dependence effects in the simulated populations, given the model settings and number of iterations applied in this study (see methods and Table 2 in the main body of the manuscript). By increasing the number of iterations to 60,000 with a 20,000 burn-in, convergence was reached in 58 populations, and we found similar patterns to those obtained with fewer iterations.

S4. Density dependence set to zero for the two oldest stages

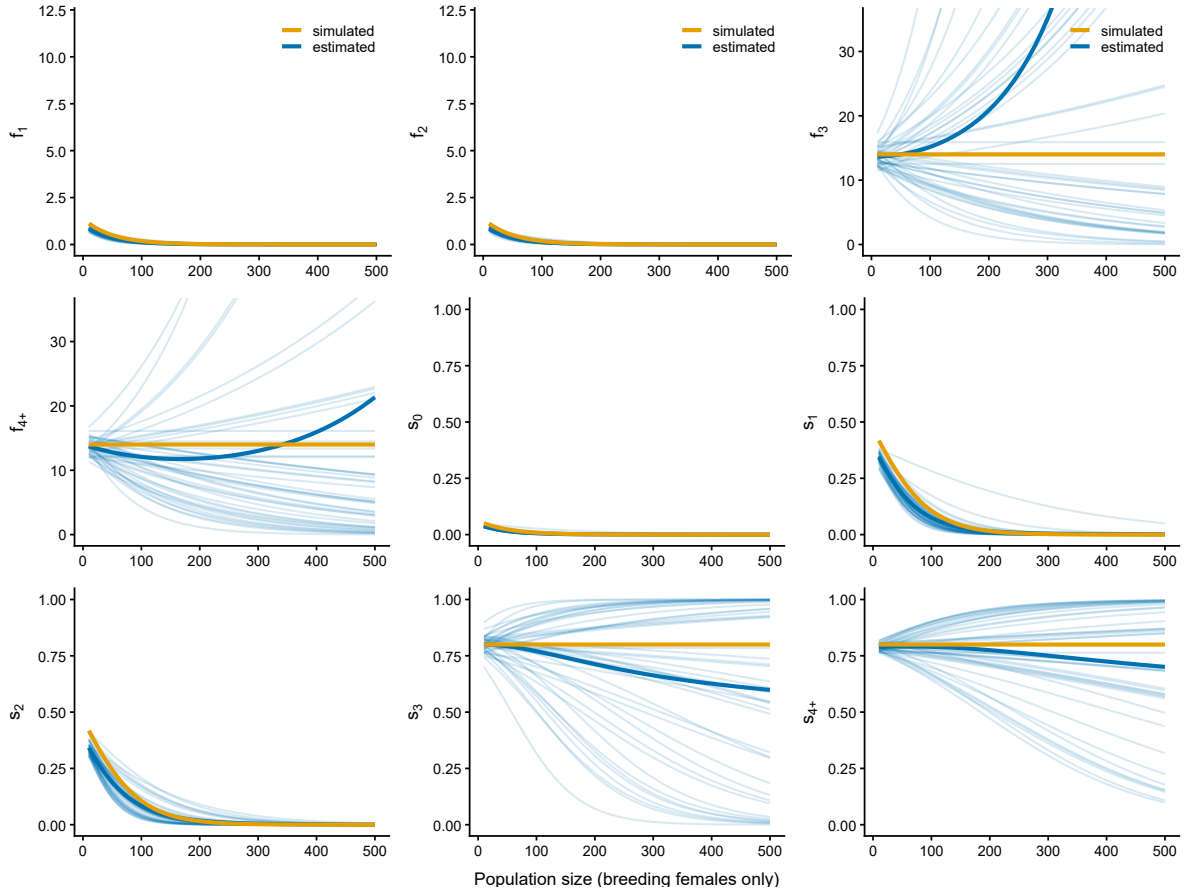

Figure S4: Density-dependent relationships for the stage-specific fecundity (f_1-f_{4^+}) and survival (s_0-s_{4^+}) estimated from scenario S9 with a four-stage model, when density dependence was set to 0 for the two oldest stages, using a 50-year time series. Orange line: simulated relationship; Bold blue line: mean of the posterior means across all converged simulations; Light blue lines: posterior mean of each individual converged simulation.

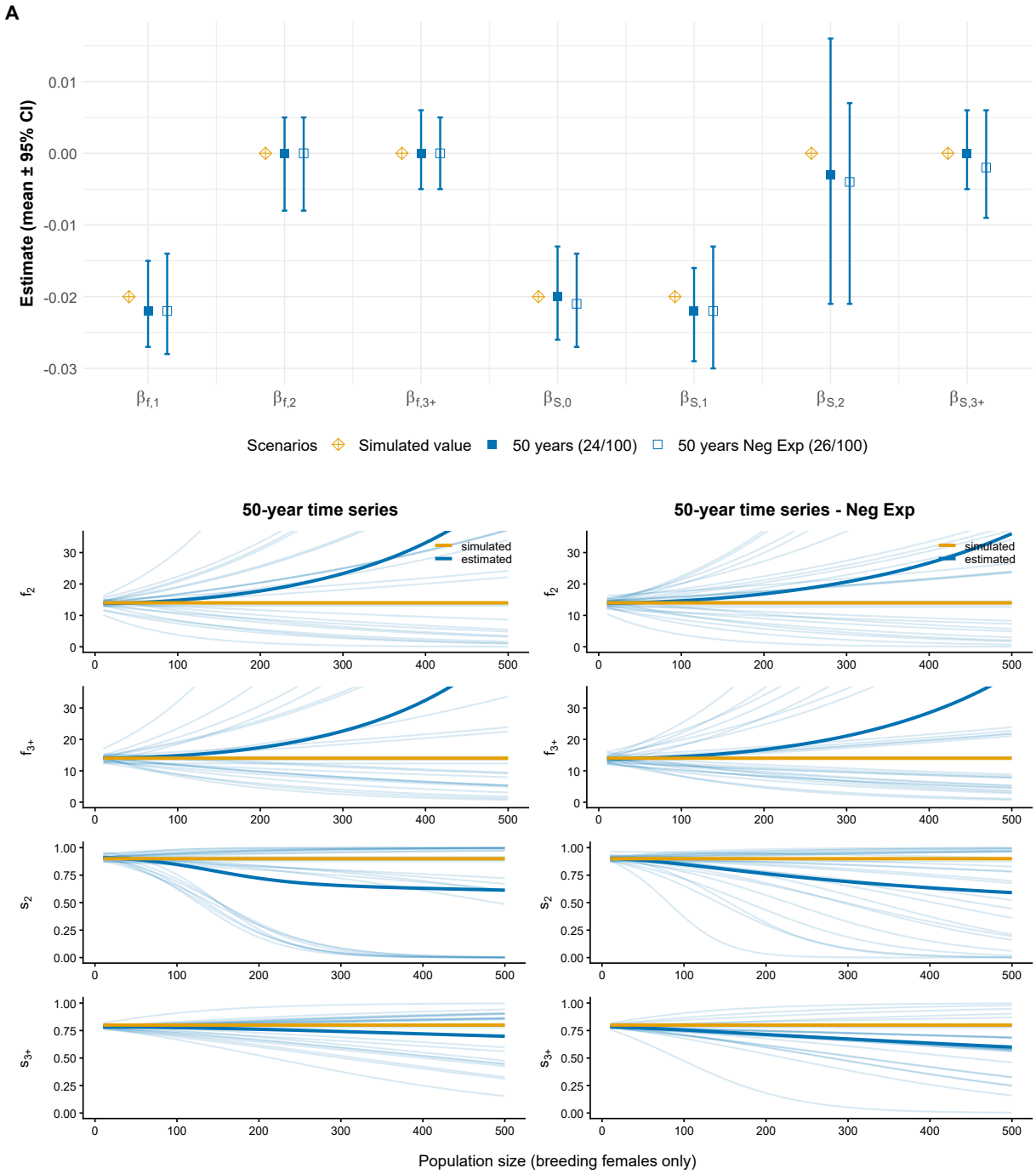

Figure S5: With a three-stage IPM model. **A.** Average posterior means of density dependence (± 95% credible intervals) for stage-specific fecundity ($\beta_{f,1}$-$\beta_{f,3+}$) and survival ($\beta_{s,0}$-$\beta_{s,3+}$) estimated based on 50-year time series when density dependence was set to 0 for the two oldest stages, and different priors for $\beta_{f,a}$ (Scenarios S19 and S21 with three-stage models). Only converged simulations were included, with the numbers of converged populations indicated in brackets (out of 100). The simulated β value for all demographic parameters was set to -0.02 (orange dashed line). Stages 0-3+ correspond to offspring, yearlings, adults of age 2 and adults of age 3+. **B.** Density-dependent relationships for a subset of four demographic parameters (f_2, f_{3+}, s_2 and s_{3+}) estimated from 50-year time series (Scenarios S19 and S21). Orange line: simulated relationship; Bold blue line: mean of the posterior means across all converged simulations; Light blue lines: posterior mean for each individual converged simulation.

- **Two additional scenarios with a three-stage IPM model and density independence for the oldest stage only, with a normal prior distribution or a negative exponential distribution for $\beta_{f,a}$.**

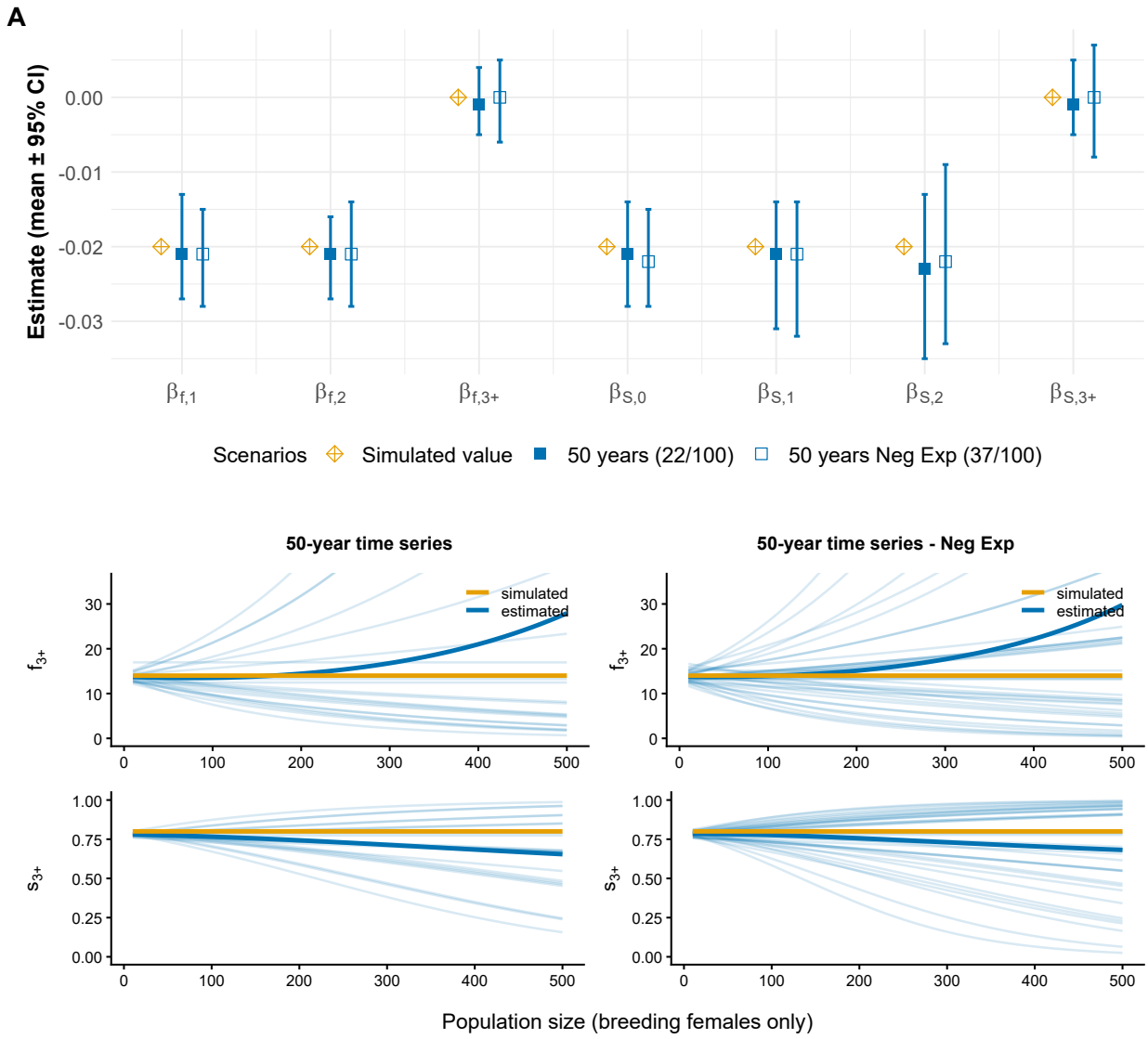

Figure S6: **A.** Average posterior means of density dependence (± 95% credible intervals) for stage-specific fecundity ($\beta_{f,1}$-$\beta_{f,3+}$) and survival ($\beta_{s,0}$-$\beta_{s,3+}$) estimated based on 50-year time series when density dependence was set to 0 for the oldest stage only, and different priors for $\beta_{f,a}$. Only converged simulations were included, with the numbers of converged populations indicated in brackets (out of 100). The simulated β value for all demographic parameters was set to -0.02 (orange dashed line). Stage classes 0-3+ correspond to offspring, yearlings, adults of age 2 and adults of age 3+.
B. Density-dependent relationships for the two density-independent demographic parameters (f_{3+} and s_{3+}) estimated from 50-year time series and different prior distribution for $\beta_{f,a}$. Orange line: simulated relationship; Bold blue line: mean of the posterior means across all converged simulations; Light blue lines: posterior mean for each individual converged simulation.

S5. Populations with increasing and decreasing trends

Populations were simulated to exhibit a decreasing or increasing temporal trend, based on the parameter values provided in Table S3. We tested six scenarios where the simulated populations displayed positive (SI1-SI3) or negative temporal trends (SD1-SD3), using time series of 15 years, 30 years or 50 years, and a four-stage IPM (Fig. S8 and S11). The strength of density dependence was simulated to be -0.005. In each case, we considered two additional scenarios, based on 30 years or 50 years of monitoring, in which strength of density dependence was set to 0 for the two oldest stages (SD4-SD5 and SI4-SI5; Fig. S9 and S12). Estimates were compared with those obtained from 30-year time series of populations with a stable trend, when the strength of density dependence for all stage-specific demographic parameters was simulated to be -0.005.

For each scenario, the 100 simulated populations were filtered according to $\log \lambda_S$ (> 0.02 or < 0.02, corresponding to increasing or decreasing trends, respectively), as well as whether the population size at the final time step exceeded or felt below twice the initial population size (for increasing or decreasing populations, respectively).

Table S3: Initial values and default parameters used to simulate each of the 100 populations with a declining or increasing trend, using a four-stage model. σ_{fa} and σ_{sa}: temporal standard deviation of stage-specific survival and fecundity, respectively; CR: capture-recapture data; maxAge: maximum number of age classes that can be identified at first capture.

Parameters	**Decreasing trend**	**Increasing trend**
Initial population vector (N_i)	$N_i = (30, 30, 30, 2)$	$N_i = (0, 5, 5, 5)$
Maximum fecundity per stage ($f_{\max}$)	$f_{\max} = (7, 7, 7, 7)$	
Maximum survival per stage ($s_{\max}$)	$s_{\max} = (0.1, 0.6, 0.6, 0.6, 0.6)$	$s_{\max} = (0.4, 0.9, 0.9, 0.8, 0.8)$
σ_{fa} and σ_{sa}	$\sigma_{fa} = 0.5$, $\sigma_{sa} = 0.4$	
Breeding probability and sex-ratio	$p_{\text{Breed}} = 0.9$, sex-ratio $= 0.5$	
Probability to find a brood	0.8	
CR – Initial capture probability	0.7	
CR – Annual recapture probability (p)	$p \sim \text{Uniform}(0.7, 0.9)$	
CR – maxAge	5	

- **Populations with declining trends**

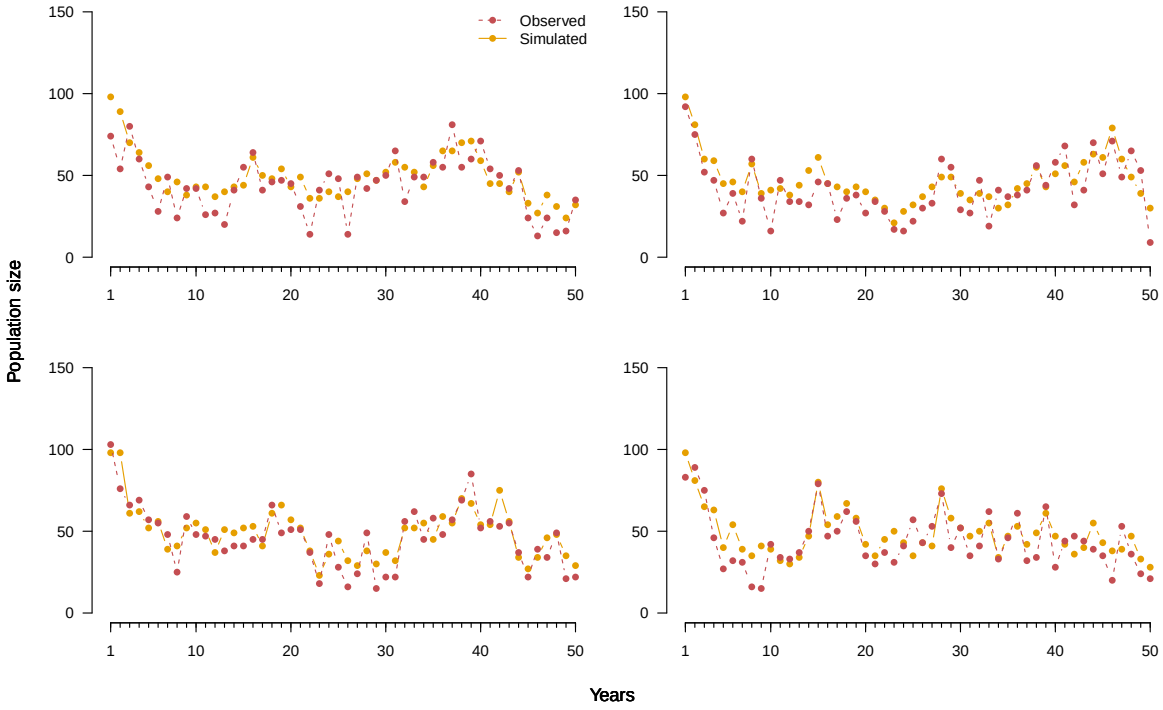

Figure S7: Simulated trajectories and observed counts for four populations over 50 years, showing a declining trend.

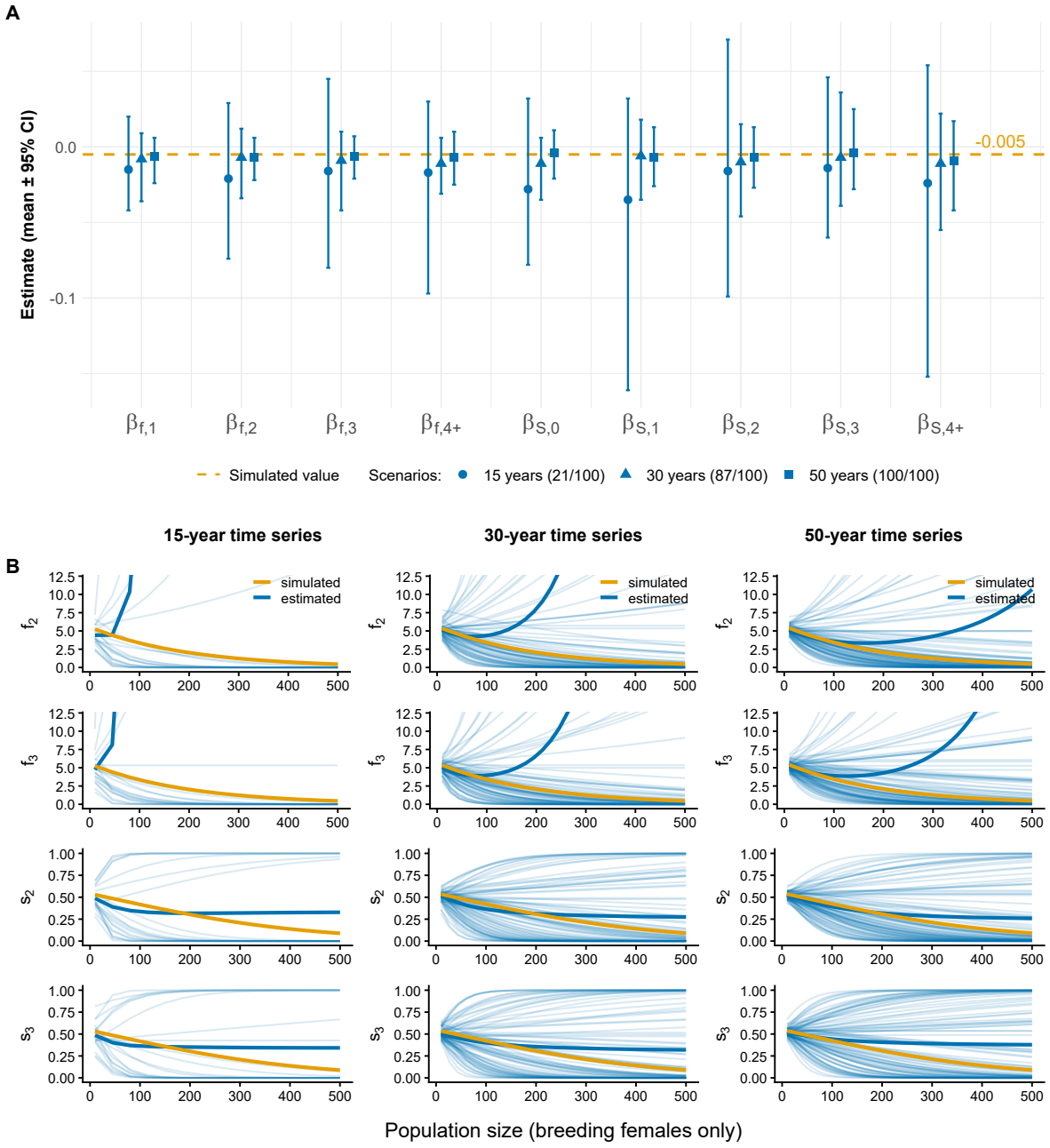

Figure S8: **A.** Average posterior means of density dependence (± 95% credible intervals) for stage-specific fecundity ($\beta_{f,1}$-$\beta_{f,4^+}$) and survival ($\beta_{s,0}$-$\beta_{s,4^+}$) estimated based on 15-, 30- and 50-year time series in decreasing populations (four-stage models). Only converged simulations were included, with the numbers of converged populations indicated in brackets (out of 100). The simulated β value for all demographic parameters was set to -0.005 (orange dashed line). Stage classes 0-4+ correspond to offspring, yearlings, 2-year-old adults, 3-year-old adults, and adults aged ≥ 4 years. **B.** Density-dependent relationships for a subset of four demographic parameters (f_2, f_3, s_2 and s_3) estimated from 15-, 30- and 50-year time series. Orange line: simulated relationship; Bold blue line: mean of the posterior means across all converged simulations; Light blue lines: posterior mean for each individual converged simulation.

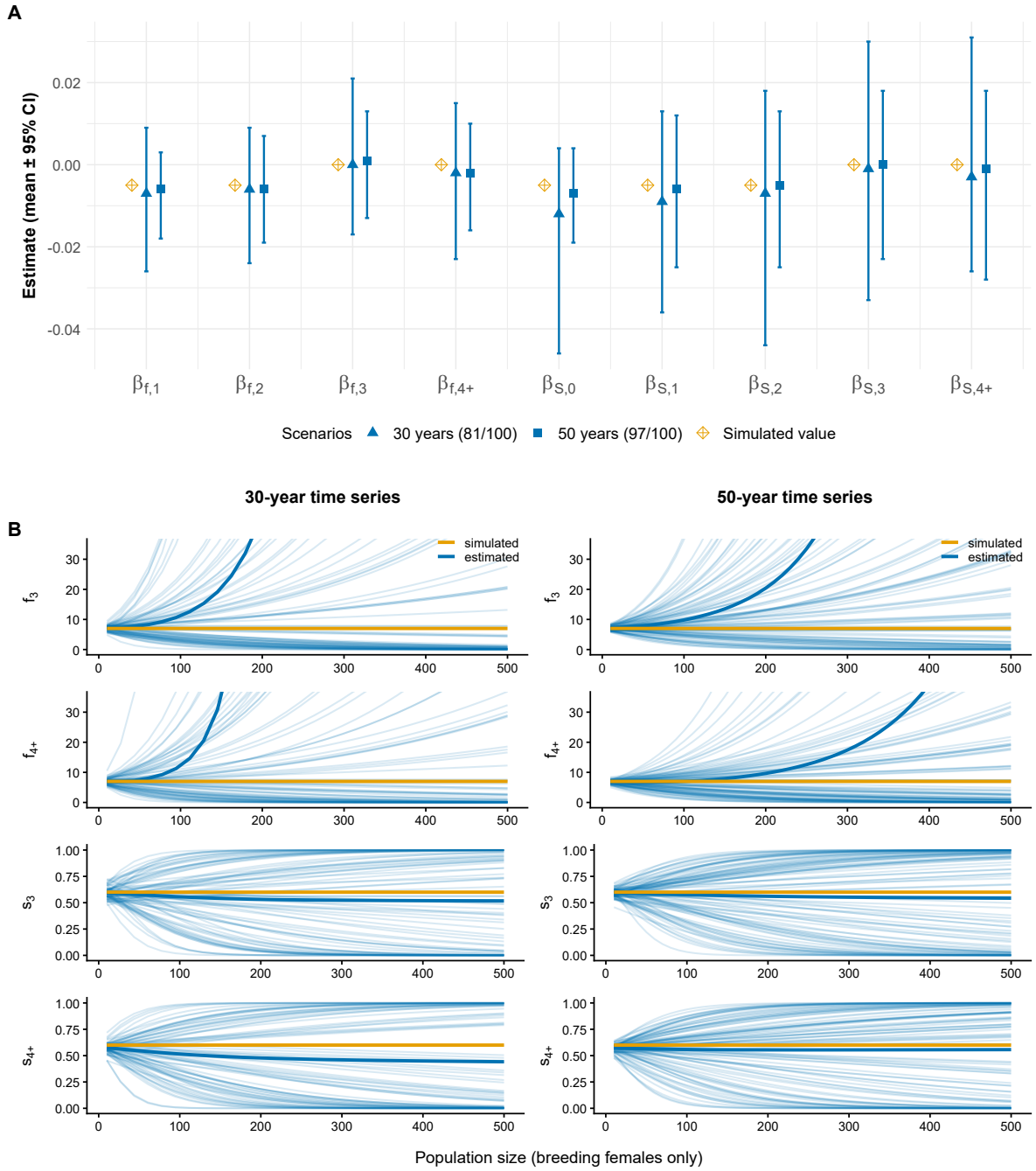

Figure S9: **A.** Average posterior means of density dependence (± 95% credible intervals) for stage-specific fecundity ($\beta_{f,1}$-$\beta_{f,4+}$) and survival ($\beta_{s,0}$-$\beta_{s,4+}$) estimated based on 30- and 50-year time series in decreasing populations (four-stage models), when demographic parameters of breeding females of age 3 and 4+ are density independent ($\beta_{f,3}$, $\beta_{f,4+}$, $\beta_{s,3}$ and $\beta_{s,4+}$ are set to 0). Only converged simulations were included, with the numbers of converged populations indicated in brackets (out of 100). The simulated β value for all density-dependent demographic parameters was set to -0.005. Stage classes 0-4+ correspond to offspring, yearlings, 2-year-old adults, 3-year-old adults, and adults aged $\geq$ 4 years. **B.** Density-dependent relationships for a subset of four demographic parameters (f_3, f_{4+}, s_3 and s_{4+}) estimated from 30- and 50-year time series. Orange line: simulated relationship; Bold blue line: mean of the posterior means across all converged simulations; Light blue lines: posterior mean for each individual converged simulation.

- **Populations with increasing trends**

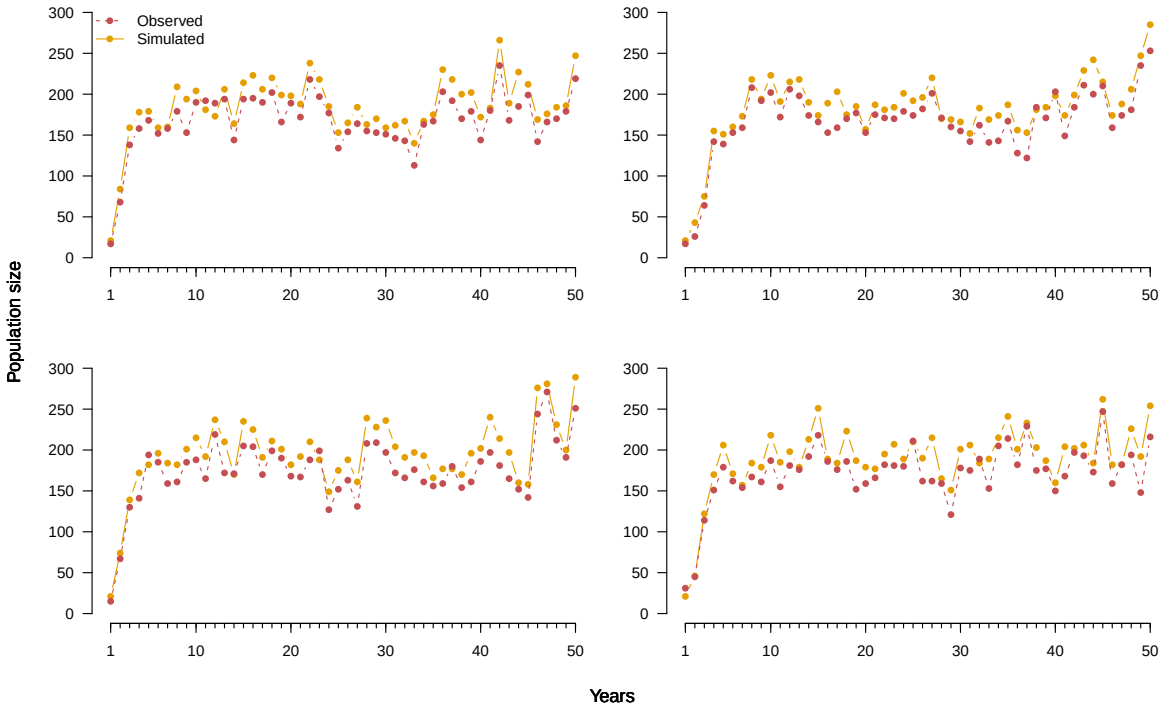

Figure S10: Simulated trajectories and observed counts for four populations over 50 years, showing an increasing trend.

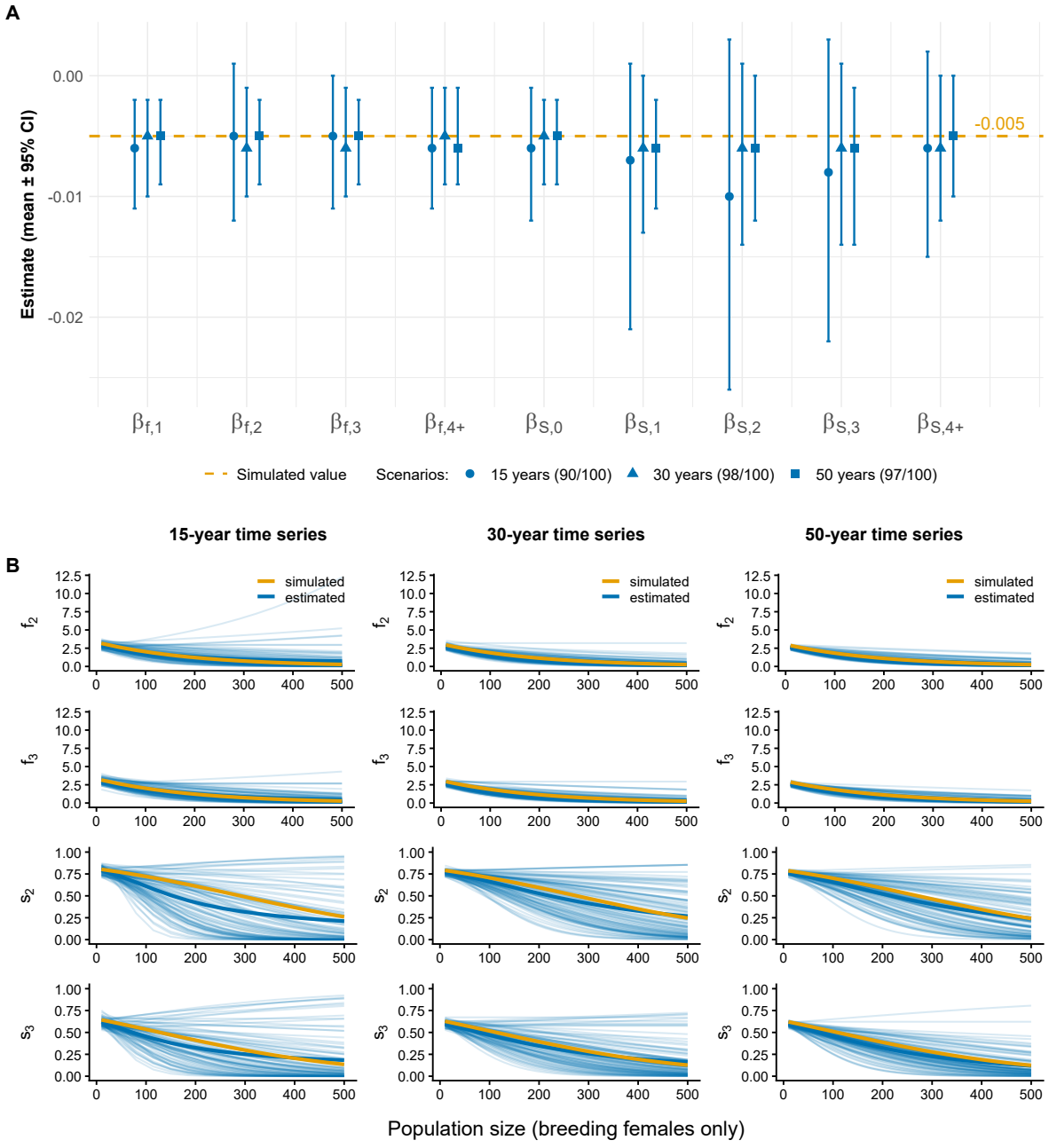

Figure S11: **A.** Average posterior means of density dependence (± 95% credible intervals) for stage-specific fecundity ($\beta_{f,1}$-$\beta_{f,4+}$) and survival ($\beta_{s,0}$-$\beta_{s,4+}$) estimated based on 15-, 30- and 50-year time series in populations with increasing trends (four-stage models). Only converged simulations were included, with the numbers of converged populations indicated in brackets (out of 100). The simulated β value for all demographic parameters was set to -0.005 (orange dashed line). Stage classes 0-4+ correspond to offspring, yearlings, 2-year-old adults, 3-year-old adults, and adults aged ≥ 4 years. **B.** Density-dependent relationships for a subset of four demographic parameters (f_2, f_3, s_2 and s_3) estimated from 15-, 30- and 50-year time series. Orange line: simulated relationship; Bold blue line: mean of the posterior means across all converged simulations; Light blue lines: posterior mean for each individual converged simulation.

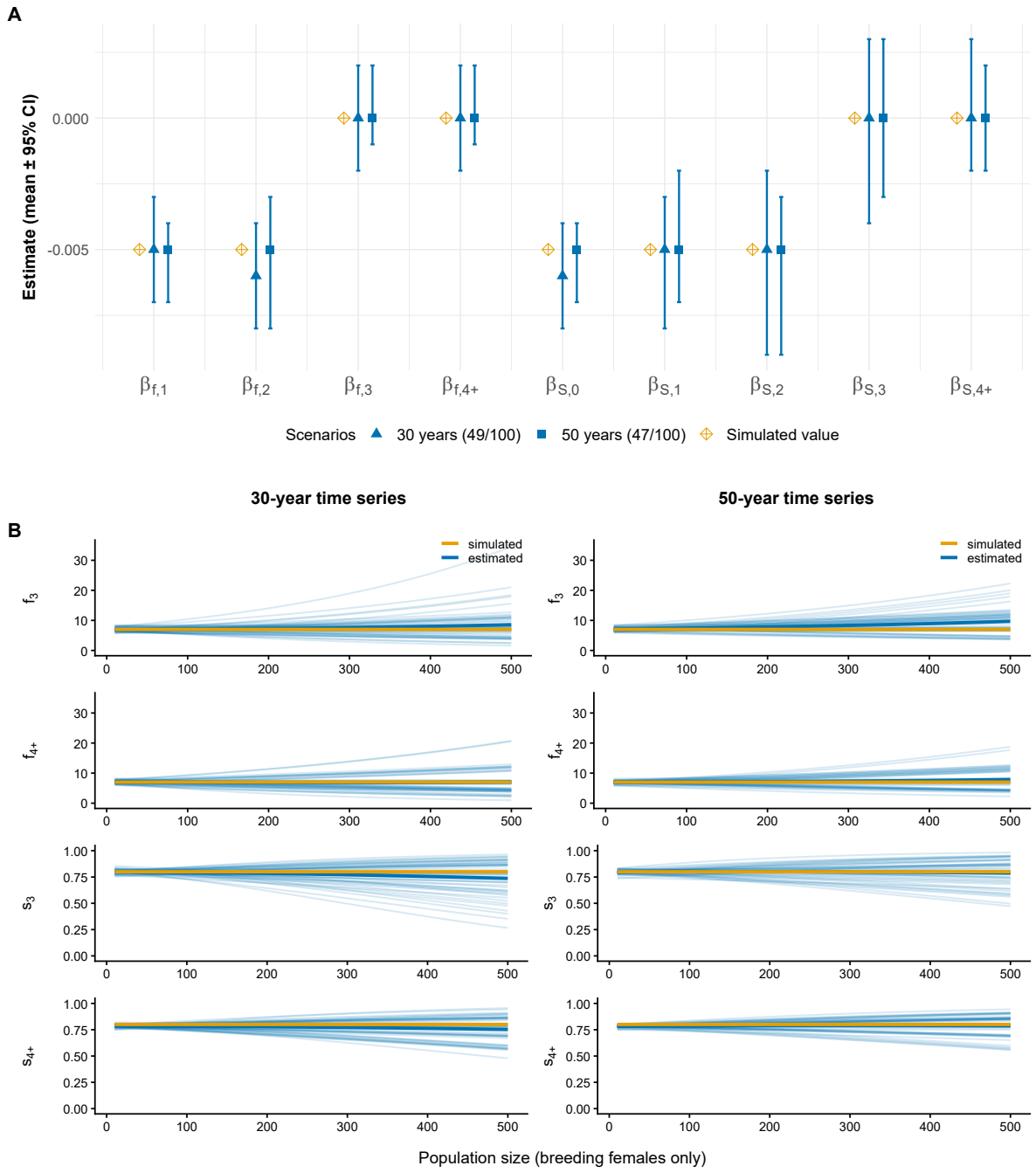

Figure S12: **A.** Average posterior means of density dependence (± 95% credible intervals) for stage-specific fecundity ($\beta_{f,1}$-$\beta_{f,4+}$) and survival ($\beta_{s,0}$-$\beta_{s,4+}$) estimated based on 30- and 50-year time series in increasing populations (four-stage models), when demographic parameters of the last two stages are density independent ($\beta_{f,3}$, $\beta_{f,4+}$, $\beta_{s,3}$ and $\beta_{s,4+}$ are set to 0). Only converged simulations were included, with the numbers of converged populations indicated in brackets (out of 100). The simulated β value for density-dependent demographic parameters was set to -0.005. Stage classes 0-4+ correspond to offspring, yearlings, 2-year-old adults, 3-year-old adults, and adults aged $\geq$ 4 years. **B.** Density-dependent relationships for a subset of four demographic parameters (f_3, f_{4+}, s_3 and s_{4+}) estimated from 30- and 50-year time series. Orange line: simulated relationship; Bold blue line: mean of the posterior means across all converged simulations; Light blue lines: posterior mean for each individual converged simulation.

S6. Density dependence in the great tit population

- Using a three-stage model

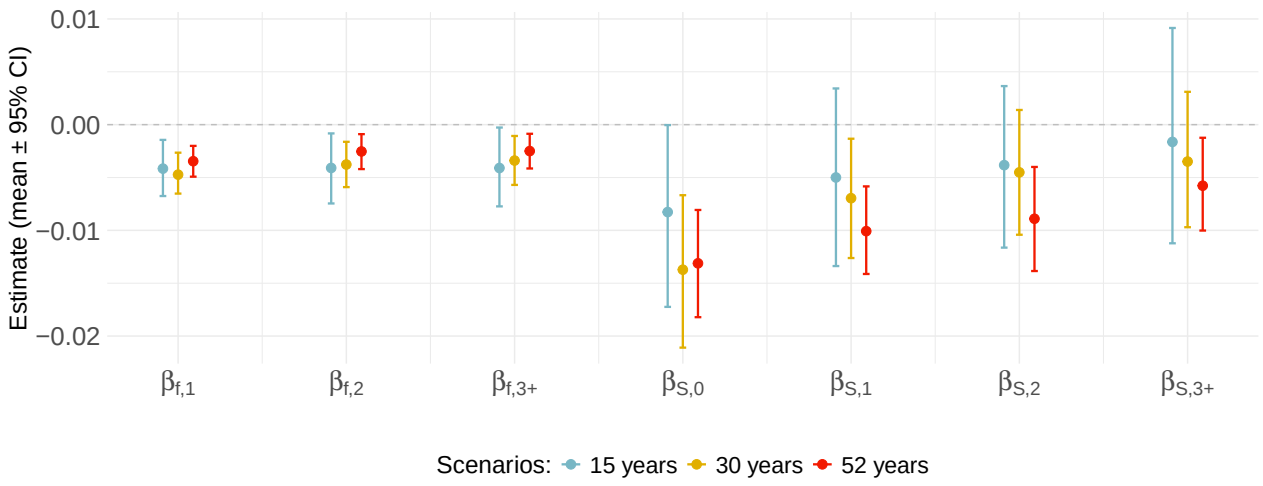

Figure S13: Posterior means of density dependence (± 95% credible intervals) of stage-specific survival ($\beta_{s,0}$-$\beta_{s,3+}$) and fecundity ($\beta_{f,1}$-$\beta_{f,3+}$) estimated in the great tit population with a three-stage model, according to the study duration from 1973 (scenarios SGT4-6).

S7. Scenarios of density dependence in populations with low recapture probability

Four scenarios were tested in which we modelled the annual recapture probability p as a random variable drawn from a uniform distribution on the interval [0.1, 0.3], and a initial capture probability of 0.5. In scenarios with high recapture probability (Tables 1-2 in the main body of the manuscript), the interval chosen for p was [0.7, 0.9] and the initial capture probability was set to 0.7. The first two scenarios correspond to populations where all demographic parameters are subject to density dependence (strength $= -0.02$), with time series lasting 30 or 50 years. In the remaining two scenarios (30- and 50-year time series), density dependence (strength $= -0.02$) was applied to the first stages, whereas it was set to zero for the final two stages (breeding females of age 3 and 4+). Except for the recapture probability, the initial parameters used to simulate populations were the same as those described in Table 2 (main body of the manuscript).

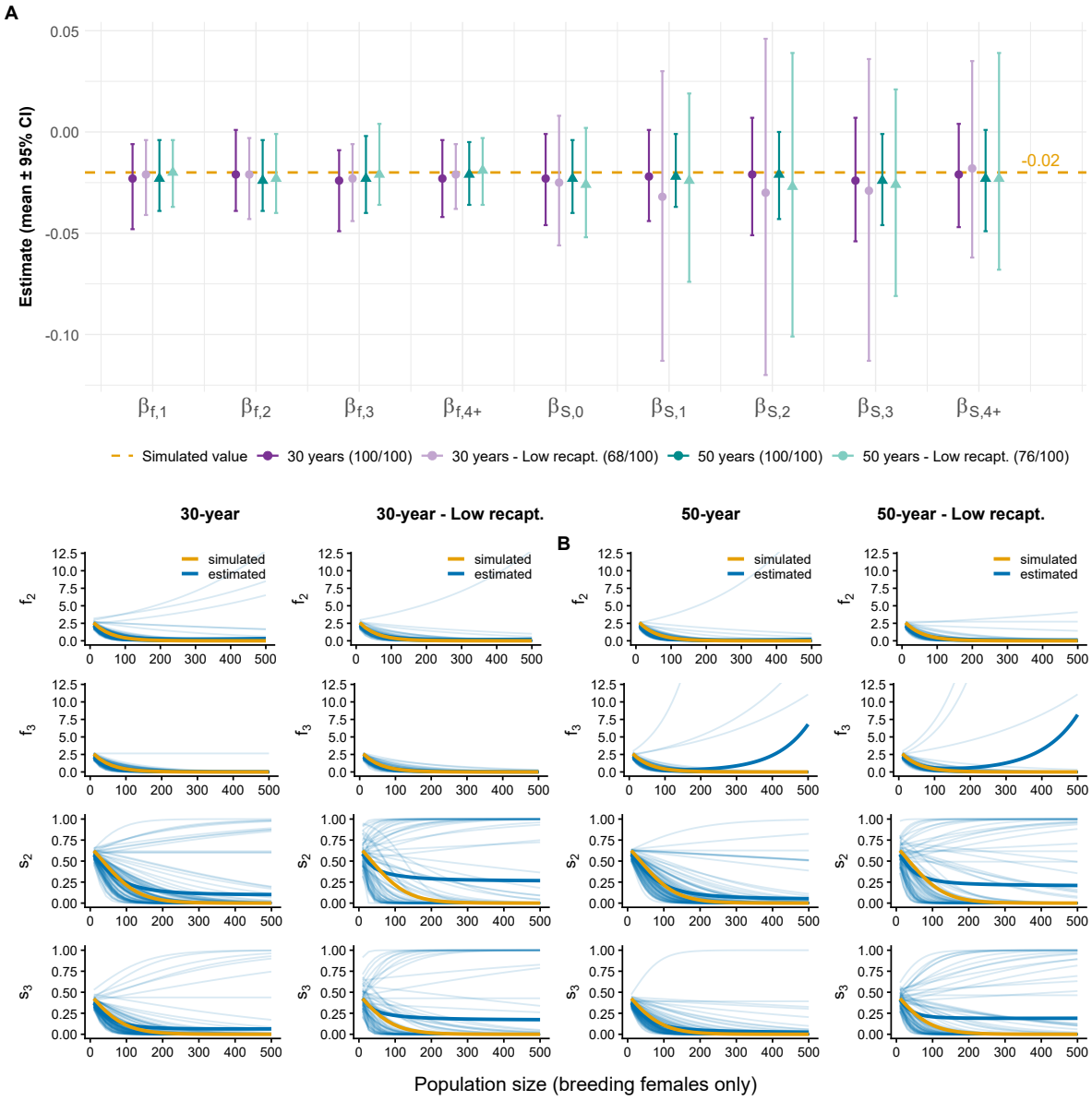

Figure S14: **A.** Average posterior means of density dependence (± 95% credible intervals) for stage-specific fecundity ($\beta_{f,1}$-$\beta_{f,4+}$) and survival ($\beta_{s,0}$-$\beta_{s,4+}$) estimated based on 30- and 50-year time series in population with a low annual recapture probability (four-stage models). Only converged simulations were included, with the numbers of converged populations indicated in brackets (out of 100). The simulated β value for density-dependent demographic parameters was set to -0.02. Stage classes 0-4+ correspond to offspring, yearlings, 2-year-old adults, 3-year-old adults, and adults aged ≥ 4 years. **B.** Density-dependent relationships for a subset of four demographic parameters (f_2, f_3, s_2 and s_3) estimated from 30- and 50-year time series of populations with a low or high recapture probability. Orange line: simulated relationship; Bold blue line: mean of the posterior means across all converged simulations; Light blue lines: posterior mean for each individual converged simulation.

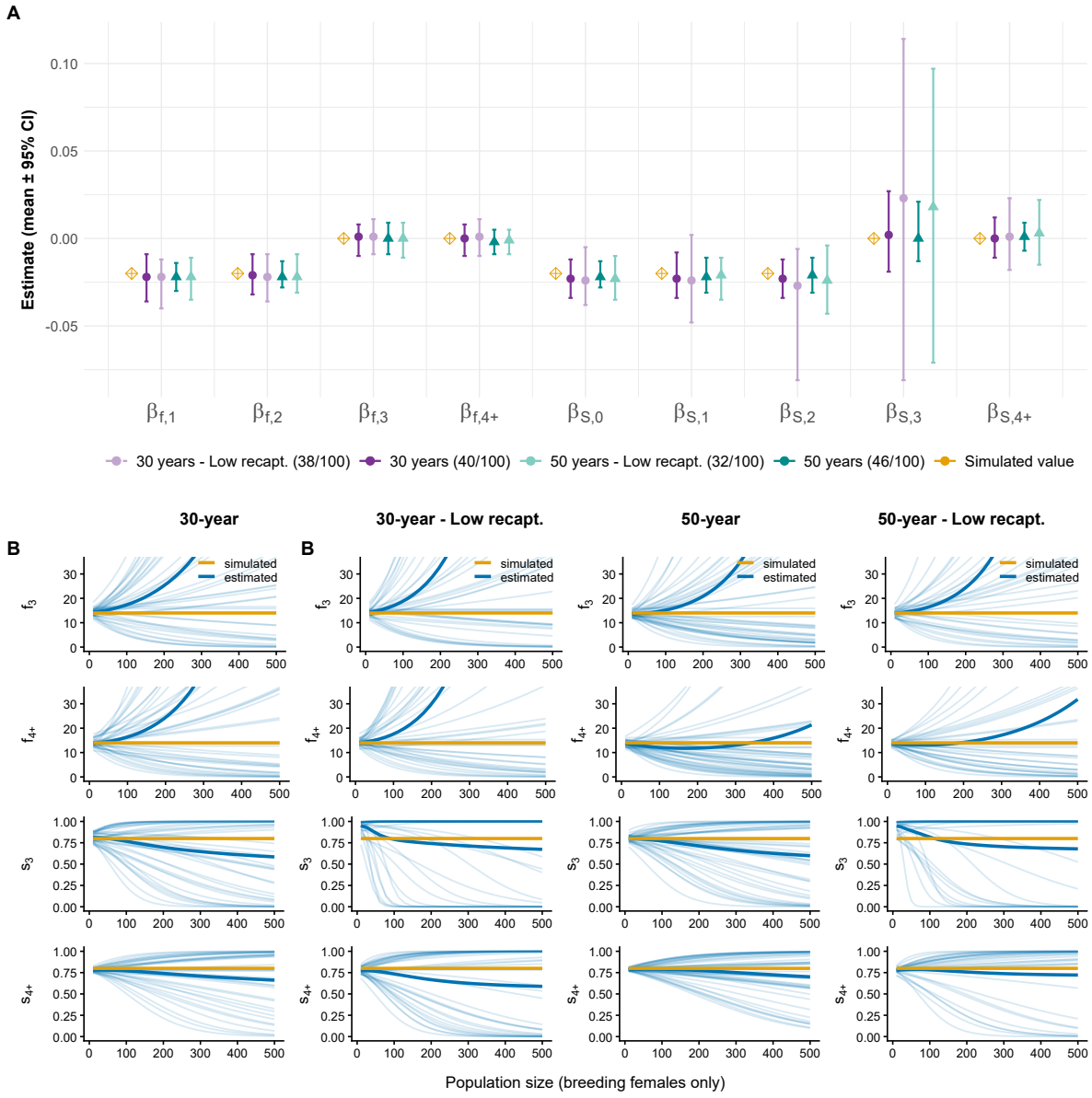

Figure S15: **A.** Average posterior means of density dependence (± 95% credible intervals) for stage-specific fecundity ($\beta_{f,1}$-$\beta_{f,4+}$) and survival ($\beta_{s,0}$-$\beta_{s,4+}$) estimated based on 30- and 50-year time series of populations with low or high annual recapture probabilities (four-stage models), when survival and fecundity of the last two stages are density independent ($\beta_{f,3}$, $\beta_{f,4+}$, $\beta_{s,3}$ and $\beta_{s,4+}$ are set to 0). Only converged simulations were included, with the numbers of converged populations indicated in brackets (out of 100). The simulated β value for density-dependent demographic parameters was set to -0.02. Stage classes 0-4+ correspond to offspring, yearlings, 2-year-old adults, 3-year-old adults, and adults aged $\geq$ 4 years. **B.** Density-dependent relationships for a subset of four demographic parameters (f_3, f_{4+}, s_3 and s_{4+}) estimated from 30- and 50-year time series of populations with a low or high recapture probability, when survival and fecundity of the last two stages are density independent. Orange line: simulated relationship; Bold blue line: mean of the posterior means across all converged simulations; Light blue lines: posterior mean for each individual converged simulation.